

Enantioselective Partitioning of Polychlorinated Biphenyls in a HepG2 Cell Culture System: Experimental and Modeling Results

Chun-Yun Zhang, Susanne Flor, Gabriele Ludewig, Hans-Joachim Lehmler*

Department of Occupational and Environmental Health, The University of Iowa, Iowa City,
Iowa 52242, United States

Corresponding Author:

Dr. Hans-Joachim Lehmler

The University of Iowa

Department of Occupational and Environmental Health

University of Iowa Research Park, B164 MTF

Iowa City, IA 52242-5000

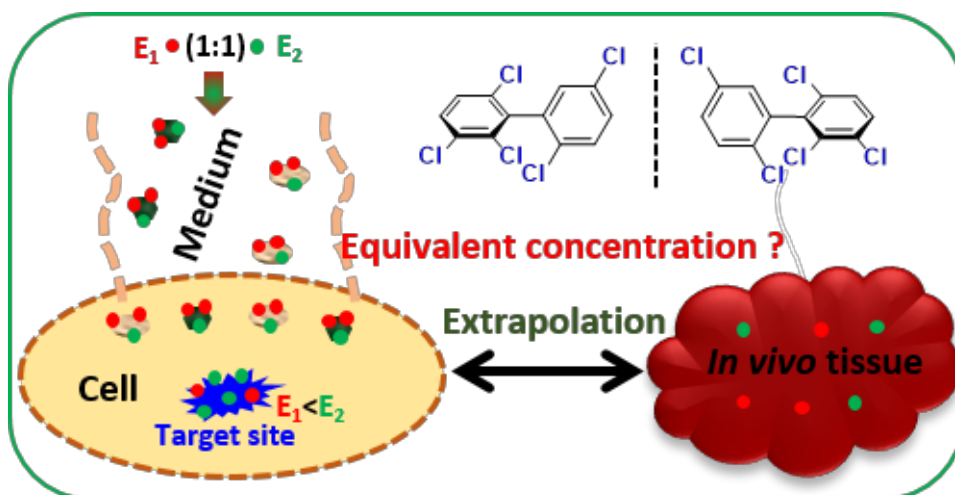
Phone: (319) 335-4981

Fax: (319) 335-4290

e-mail: hans-joachim-lehmler@uiowa.edu

ABSTRACT

Cell culture studies are used to study the toxicity of polychlorinated biphenyls (PCBs); however, it is typically unknown how much PCB enters the cells. We investigated the partitioning of chiral PCBs (PCB 91, PCB 95, PCB 132, or PCB 136) in the human hepatoma HepG2 cell line. We used a computational model for the *in vitro* to *in vivo* extrapolation (IVIVE) of PCB levels. HepG2 cells were incubated with PCBs for 72 h. PCB levels were quantified in cells, media, and cell culture dishes. PCBs were present in cell culture medium (60.7-88.8 %), cells (8.0-14.6 %), and dishes (2.3-7.8 %), and displayed atropisomeric enrichment in cells (enantiomeric fraction [EF]=0.55-0.77) and dishes (EF=0.53-0.68). The free PCB concentration in media, estimated using polyparameters linear free energy relationships (PP-LFERs) and a composition-based model, was used to extrapolate from the nominal PCB concentration used *in vitro* to PCB tissue levels and *vice versa*. This approach allows for an IVIVE but does not account for the atropselective partitioning of chiral PCBs between medium and cells. Because PCB atropisomers differ in their toxicities, the atropselectively partitioning of PCBs between culture medium and cells needs to be considered when interpreting cell culture-derived data.



INTRODUCTION

Polychlorinated biphenyls (PCBs) are a class of persistent organic pollutants (POPs).¹ Because PCBs pose an environmental and human health hazard, the Stockholm Convention has banned the production of PCBs worldwide. Besides, parties to the Convention have committed to stop the use of PCBs in technical applications, such as transformers and capacitors, by 2025 and to dispose of legacy PCBs in an environmentally sound manner by 2028.² However, some PCBs are still produced unintentionally and can be found in consumer products, such as paint and resins.³⁻⁵ Moreover, PCBs are still present in building materials and can contaminate the indoor air of buildings, such as schools.^{6,7} Biomonitoring studies demonstrate that PCB levels in human food, human serum and environmental samples, such as fish livers, only slightly decreased over the last two decades.⁸⁻¹⁰ Overall, PCBs represent a significant and current public health concern.

Exposure to PCBs has been linked to a range of adverse human health outcomes, including cancer, immunotoxicity, cardiovascular disease, and developmental neurotoxicity.¹¹ PCB congeners with multiple *ortho* substituents have been implicated in the developmental neurotoxicity of PCBs.¹² Several of these neurotoxic PCB congeners display axial chirality and exist as stable rotational isomers, or atropisomers, which are non-superimposable mirror images of each other. Chiral PCB congeners are enantioselectively metabolized to potentially neurotoxic hydroxylated and sulfated metabolites,^{13, 14} resulting in an atropisomeric enrichment of both the parent PCB and its metabolites in environmental samples, wildlife, and humans.^{13, 15} These findings are toxicologically relevant because PCB atropisomers can atropselectively affect biological targets in the liver and brain. PCB atropisomers atropselectively affect the expression of drug-metabolizing enzymes in the rat liver,^{16, 17} and bind atropselectively to cytochrome P450

enzymes.¹⁸ Pure atropisomers of PCBs 95 and 136 selectively affect endpoints involved in PCB developmental neurotoxicity by mechanisms involving ryanodine receptors (RyRs).¹⁹⁻²¹

These *in vitro* models are a powerful tool to study chiral PCBs, either as a racemic mixture or individual atropisomers. However, it remains challenging to extrapolate from the nominal PCB concentrations used in *in vitro* studies to *in vivo* tissue concentrations and *vice versa*. We posit that the free concentration of PCBs (i.e., the PCB concentration not bound to proteins and lipids) can be used for IVIVE because only the free PCB concentration is available for partitioning into or out of cells.^{22, 23} Because it is challenging to measure the free concentration of chemicals experimentally, several models have been developed to connect their nominal concentration to the free concentration using the quantities and sorptive capacities of each biological component (i.e., protein, lipid, and water).^{22, 24-26} The free concentration in the aqueous phase (C_{free}) can be calculated from nominal concentration ($C_{nominal}$) using the general mass balance equation as follows:

$$C_{free} = \frac{C_{nominal} V_{medium}}{\sum K_{i/water} V_i} \quad (1)$$

where i represents the sorptive components, including protein, lipid, water, etc. When the sorptive component i is water, the partitioning coefficient $K_{i/water}$ equals to 1. V_{medium} is the volume of medium and V_i is the volume of component i .

The C_{free} calculated for the *in vitro* bioassay can subsequently be used for IVIVE to estimate tissue levels (C_{tissue}) *in vivo* with the following equation:

$$C_{tissue} = C_{free} \sum K_{i/water} f_i \quad (2)$$

where f_i is the volume fraction of the biological component i *in vivo*. The quantities of the biological components *in vitro* and *in vivo* can be determined experimentally or are available from

the literature.^{22, 27} In addition, $K_{i/water}$ can be measured or estimated from the octanol/water partition coefficient (K_{ow})^{23, 24} or PP-LFERs.^{22, 27} These data are readily available for all 209 PCB congeners.²⁸

This study characterized the partitioning of PCB 91, PCB 95, PCB 132, and PCB 136, four environmentally and toxicologically relevant chiral PCBs,^{13, 14} in a HepG2 cell culture model in the absence of detectable PCB metabolism. The free concentration of PCBs in the cell culture model was estimated, either based on the PCB levels measured in the medium at the endpoint or added in the beginning using a PP-LFER composition-based model. Because the experiment-based and theoretical free PCB concentrations showed a reasonable agreement, the PP-LFER-based free concentrations were used to extrapolate the nominal PCB concentration of all 209 PCB congeners in the HepG2 cell culture assays to tissue levels and *vice versa*. While this approach allows a straightforward IVIVE, it does not account for the enantioselective partitioning of chiral PCBs between medium and cells. Importantly, typical concentrations used in cell culture studies are frequently higher than equivalent tissue concentrations.

EXPERIMENTAL SECTION

Materials. 2,2',3,5'-Pentachlorobiphenyl (PCB 95), 2,2',3,3',6,6'-hexachlorobiphenyl (PCB 136), 4'-chloro-3'-fluoro-4-sulfooxy-biphenyl (3-F,4'-PCB 3 sulfate, surrogate of PCB metabolites), 4'-chloro-3'-fluoro-4-hydroxy-biphenyl (3-F,4'-OH-PCB 3, surrogate of PCB metabolites) were synthesized and authenticated as previously described.^{29, 30} 2,2',3,4'-Pentachlorobiphenyl (PCB 91), 2,2',3,3',4,6'-hexachlorobiphenyl (PCB 132), 2,3,4',5,6-pentachlorobiphenyl (PCB 117, recovery standard for PCBs), 2,3,3',4,5,5'-hexachlorobiphenyl-4'-ol (4'-OH-PCB 159, recovery standard for OH-PCBs) and 2,2',3,4,4',5,6,6'-octachlorobiphenyl (PCB 204, internal standard) were purchased from AccuStandard, Inc. (New

Haven, CT, USA). Analytical standards of OH-PCBs and methylated derivatives of OH-PCBs were synthesized and authenticated as reported earlier (for additional information, see Table S1).³¹ Solutions of diazomethane in diethyl ether were prepared from *N*-methyl-*N*-nitroso-*p*-toluenesulfonamide (Diazald) using an Aldrich mini Diazald apparatus (Milwaukee, WI, USA).

Sulfatase (type H-2 from *Helix pomatia*, ≥ 2000 units/mL) for the deconjugating of potential hydroxylated PCB conjugates and resazurin sodium salt were purchased from Sigma-Aldrich (St Louis, MO, USA). Phenol red-free minimum essential medium (MEM), fetal bovine serum (FBS), L-glutamine, glucose solution, penicillin/streptomycin (P/S), Dulbecco's phosphate-buffered saline (PBS), trypsin-EDTA, Costar 6- and 24-well plates, as well as dimethyl sulfoxide (DMSO), were obtained from Thermo Fisher Scientific (Radnor, PA, USA).

HepG2 cells were purchased from the American Type Culture Collection (ATCC; Manassas, VA, USA). The authenticity of the human hepatocellular carcinoma cell line HepG2 was confirmed by analysis of genomic DNA conducted by the University of Arizona Genetics Core (Arizona Research laboratories, Tucson, AZ, USA). The HepG2 cells used in this study were between passages 18 through 35. Cells were maintained in complete medium (MEM supplemented with 10 % FBS, 100 U/mL penicillin, 100 μ g/mL streptomycin, and 2 mM l-glutamine) in a humidified incubator with 5% CO₂ at 37 °C. Exposure medium contained MEM with 10 % FBS was supplemented with 100 U/mL penicillin, 100 μ g/mL streptomycin, and 2 mM l-glutamine. PCBs (i.e., PCB 91, PCB 95, PCB 132, and PCB 136) were dissolved in DMSO. The final concentration of DMSO in the medium did not exceed 0.1 % (v/v). This DMSO concentration did not have any effect on cell viability.

PCBs exposure of HepG2 cells. HepG2 cells (6×10^6 /well) were seeded into 6-well plates with 3 mL complete medium per well. After 48 h attachment, cells were exposed in triplicates to

0.25, 1 or 10 μ M of the racemic PCB 91, PCB 95, PCB 132, and PCB 136 (0.1 % DMSO) in exposure medium (3 mL). The control group was exposed to 0.1 % DMSO in triplicates in the exposure medium. After a 72 h incubation, the medium was carefully transferred into weighted glass vials, and the cells were washed once with PBS (1 mL). This solution was combined with the exposure medium. The cells were harvested into PBS (1mL) with a rubber policeman and added into a weighted glass vial. The wells were washed once with PBS (1 mL), and the washing solution was combined with the cell suspension. All vials were stored at -20 °C until analysis. The plates were wrapped in aluminum foil and stored at 4 °C until analysis. The cytotoxicities of PCBs at concentrations of 0.25 μ M and 10 μ M are summarized in Fig. S1.

In separate experiments, cell-free plates with 10 μ M of the racemic PCBs in exposure medium or 0.25 μ M of the racemic PCBs in MEM were also incubated for 72 h, and samples were processed as described above to study the partitioning of PCBs in the cell culture wells in the absence of cells.

Extraction of PCBs and their metabolites from media, cell pellets, and dishes. Depending on the PCB concentrations, different extraction workflows were used for media, cell pellets, and dish samples (Fig. S2). The extraction of media samples (0.25 and 10 μ M) and cell pellets samples (0.25 μ M only) was described previously, with minor modification.³²⁻³⁴ Briefly, samples were spiked with PCB 117 (100 ng in isooctane) and 4'-OH-PCB 159 (50 ng in methanol) and acidified with hydrochloric acid to protonate OH-PCBs (6 M, 1 mL). The samples were extracted with hexane/MTBE (1:1 v/v, 5 mL), 2-propanol (5 mL) was added, and samples were re-extracted with hexane (3 mL). The combined organic phases were washed with a potassium chloride solution (1 % w/v, 4 mL), the organic phase was evaporated to dryness under a gentle stream of nitrogen, and the sample was reconstituted in hexane (1 mL). The extract was

derivatized using diazomethane in ethyl ether (0.5 mL) overnight at 4 °C,³⁵ and subjected to sulfur removal and sulfuric acid clean-up steps as described.^{36, 37} After extraction with hexane/MTBE, the medium samples (10 µM PCB exposure groups only) were deconjugated with sulfatase (type H-2 from *Helix pomatia*) as described in the Supporting Information to assess the presence of sulfate or glucuronide conjugates in the cell culture media. PCB 204 (100 ng) was added as an internal standard (volume corrector) before the gas chromatographic analysis.^{36, 37}

Cell culture dishes were allowed to dry, PCB 117 (100 ng in isooctane) was added, and all dishes were washed twice with hexane (4 mL and 3 mL).²⁰ The hexane phase was cleaned up as described above for media and cell pellets samples.

Untargeted analyses were performed with media samples from the 1 µM PCB exposure groups. Briefly, media samples were extracted with acetonitrile, and the resulting extracts were screened for the presence of PCB metabolites by Ultra-Performance Liquid Chromatography-Quadrupole Time-of-flight Mass Spectrometry (UPLC-QToF-MS) as described in the Supporting Information.

Quantitative gas chromatographic analyses of PCBs and their metabolites. Quantitative analysis of PCBs and OH-PCBs (as methylated derivatives) in sample extracts was carried out on an Agilent 7890A gas chromatograph (GC) equipped with an SPB-1 capillary column (60 m length, 250 µm inner diameter, 0.25 µm film thickness; Supelco, St Louis, MO, USA) and a ⁶³Ni-micro electron capture detector (µECD) as previously reported.^{32, 33} Helium was used as carrier gas with a constant flow rate of 2 mL/min. The temperature program was as follows: initial temperature 50 °C for 1 min, 30 °C/min to 200 °C, 1 °C/min to 250 °C, 10°C/min to 280 °C, and hold for 3 min. The PCBs were identified based on their retention time, with relative

retention times (RRT) being within 0.5 % of the RRT of the respective PCBs standard.³⁸ PCBs were quantified with the internal standard using the relative response factors in both samples and the reference standard mixture. PCB levels were corrected for the recovery of the surrogate recovery standard to account for any loss of PCBs during the extraction. The hydroxylated PCB metabolites (as methylated derivatives) listed in Table S1 were not detected in any sample.

Atropselective gas chromatographic analyses of PCBs. Enantioselective analyses of PCBs were employed by an Agilent 6890 gas chromatograph (GC) equipped with a ⁶³Ni-μECD detector and CP-Chirasil Dex CB (CD) (25 m length, 250 μm inner diameter, 0.25 μm film thickness; Agilent, Santa Clara, CA, USA) or Cyclosil-B (CB) (30 m length, 250 μm inner diameter, 0.25 μm film thickness; Agilent) capillary columns.³⁹⁻⁴¹ The flow rate of the carrier gas, helium, was 3 mL/min.^{34, 39, 40, 42} The temperature program for the atropselective analysis of PCB 91, PCB 95 and PCB 136 was as follows: initial temperature 50 °C for 1 min, 10 °C/min to 140 °C, hold for 170 min, 15 °C/min to 200 °C, and hold for 20 min. The column temperature program for the atropselective analysis of PCB 132 was as follows: initial temperature 50 °C for 1 min, 10 °C/min to 160 °C, hold for 140 min, 15 °C/min to 200 °C, and hold for 20 min. The enantiomeric fraction (EF) was determined with the drop valley method and calculated as $EF = \frac{\text{Area } E_1}{\text{Area } E_1 + \text{Area } E_2}$, where Area E₁ and Area E₂ are the peak areas of the atropisomer eluting first and second on the chiral column.^{34, 39, 40, 42} A summary of the EF values on different columns is provided in Table S2.

Quality assurance/quality control (QA/QC). The responses of the electron capture detector were linear from 1 to 1000 ng/mL for all the analytes. Method blanks and matrix blanks (media, cell pellets, and dishes) were analyzed in parallel with all samples. Besides, samples from control incubations were analyzed in parallel, including blank incubations with HepG2 cells exposed to

0.1 % DMSO only and blank, cell-free incubations containing only MEM medium and 0.1 % DMSO. The quality assurance/quality control (QA/QC) data, including the limits of detection (LODs) of PCBs, the PCB background levels calculated from the matrix blanks, the recoveries of surrogate standard (PCB 117) for all samples, resolution of the PCB atropisomers, and the EF values of the racemic standards, are summarized in Table S3.

Equilibrium partitioning model in the cell culture system. Building on a published, composition-based model,²² we predicted the partitioning of the PCBs in the cell culture system by accounting for the well-documented differences in the partitioning of PCBs into different lipid classes (Fig. S3).^{43, 44} In our four-component model, both the cell and medium compartments were assumed to consist of albumin protein, membrane lipid, storage lipid, and water. Assuming a partition equilibrium between the compartments in the cell culture system, the free concentration of PCBs can be calculated from the initial amount of PCB added into the incubation (m_0) and the sorptive capacities of the biological components in both medium and cells using the following equation (for more details, see the Supporting Information):

$$C_{free} = \frac{m_0}{K_{ap,w}(V_{m,ap}+V_{c,ap})+K_{ml,w}(V_{m,ml}+V_{c,ml})+K_{sl,w}(V_{m,sl}+V_{c,sl})+V_{m,w}+V_{c,w}} \quad (3)$$

where $K_{ap,w}$, $K_{ml,w}$ and $K_{sl,w}$ are the partition coefficients of PCBs between protein and water, membrane lipid and water, and storage lipid and water, respectively; $V_{m,ap}$, $V_{m,ml}$, $V_{m,sl}$ and $V_{m,w}$ are the phase volumes of albumin protein, membrane lipid, storage lipid and water in the medium; $V_{c,ap}$, $V_{c,ml}$, $V_{c,sl}$ and $V_{c,w}$ are the phase volumes of protein, membrane lipid, storage lipid, and water in cells. The m_0 values used for the model calculations were corrected by subtracting the measured levels of PCBs absorbed to the cell culture dishes. The partition coefficients of PCBs used for the calculations were obtained from established PP-LFERs.²⁷ The

solvation parameters used for the PP-LFERS²⁸ and other parameters needed for the model predictions were obtained from published literature values (Table S4).^{22, 45, 46}

For comparison, the free concentration of PCBs in the cell culture system was calculated from the measured PCBs levels in medium (m_{medium}) and the sorptive capacities of the biological components in medium (for more details, see the Supporting Information), i.e.,

$$C_{free} = \frac{m_{medium}}{K_{ap,w}V_{m,ap} + K_{ml,w}V_{m,ml} + K_{sl,w}V_{m,sl} + V_{m,w}} \quad (4).$$

***In vitro-in vivo* extrapolation of PCB levels.** The C_{free} values from the cell culture experiments were used to calculate equivalent PCBs levels in the liver and plasma with a composition-based model for describing *in vivo* systems. In this model, the biological components in both plasma and liver are albumin proteins, muscle proteins, storage lipids, membrane lipids, and water.²⁷ The equivalent PCBs levels in liver and plasma can be expressed as (for more details, see the Supporting Information)

$$C_{liver} = C_{free}(K_{ap,w}f_{l,ap} + K_{mp,w}f_{l,mp} + K_{ml,w}f_{l,ml} + K_{sl,w}f_{l,sl} + f_{l,w}) \quad (5)$$

and

$$C_{plasma} = C_{free}(K_{ap,w}f_{p,ap} + K_{mp,w}f_{p,mp} + K_{ml,w}f_{p,ml} + K_{sl,w}f_{p,sl} + f_{p,w}) \quad (6)$$

respectively. $K_{mp,w}$ is the partition coefficient of PCBs between muscle protein and water. $f_{l,ap}$, $f_{l,mp}$, $f_{l,ml}$, $f_{l,sl}$ and $f_{l,w}$ are the volume fractions of albumin proteins, muscle proteins, membrane lipids, storage lipids, and water in the liver, respectively. $f_{p,ap}$, $f_{p,mp}$, $f_{p,ml}$, $f_{p,sl}$ and $f_{p,w}$ are the volume fractions of albumin proteins, muscle proteins, membrane lipids, storage lipids, and water in plasma, respectively. The partitioning coefficients of PCBs used for the calculations were obtained from established PP-LFERS.²⁷ All the volume fractions were obtained from literature data.²⁷

RESULTS AND DISCUSSION

Characterization of the PCBs metabolism in HepG2 cells. Although HepG2 cells can metabolize environmental pollutants, such as PAHs and others,⁴⁷⁻⁴⁹ it is also well documented that, compared to primary human hepatocytes and hepatospheres, HepG2 cells express lower levels of xenobiotic processing enzymes,⁵⁰ including cytochrome P450 isoforms involved in the metabolism of chiral PCBs.⁴⁰ Cells were exposed for 72 h to these four PCB congeners (0.25 μ M or 10 μ M) to assess if HepG2 cells can metabolize PCB 91, PCB 95, PCB 132 and PCB 136. Cell culture media and cell pellets were extracted and analyzed for PCB metabolites using targeted and untargeted approaches (Fig. S2). No hydroxylated, sulfated, glucuronidated, or other metabolites were detected in any sample. This finding is not surprising because PCB metabolism decreases with increasing degree of chlorination and is expected to be relatively low for the penta- and hexa-chlorinated PCB congeners investigated.⁵¹

Quantitative distribution of PCBs in the HepG2 cell culture system. We quantified the PCBs levels in cell culture media, cells, and dishes in the absence of detectable PCB metabolism after PCBs incubation with and without HepG2 cells for 72 h (Fig. 1). Large percentages (60 to 89 %) of PCBs were recovered from the cell culture medium supplemented with 10 % FBS. Only 7.9 to 14.7 % of the PCBs were associated with the cell pellets. Approximately 6 % (2.3 to 7.8 %) of PCBs were absorbed onto the cell culture dishes, both for incubations with and without cells. The percentage of the two hexachlorinated congeners was higher in the medium than the percentage of the pentachlorinated congeners. This finding is consistent with an increasing affinity of PCBs for serum proteins, such as albumin, with an increasing degree of chlorination. Similarly, an *in vitro* study showed that the binding affinity of PCBs for binding site II of albumin, the major protein in FBS, increases with an increase in the number of chlorine atoms.⁵²

The PCB mass ratios between cell pellets : media : dishes were 1 : 4.9 : 0.54 for pentachlorinated congeners and 1 : 8.6 : 0.37 for hexachlorinated congeners, respectively. These ratios are comparable to earlier studies. For example, the PCB ratios between cell pellets : media : dishes for a lower chlorinated PCB congener, PCB 11, were 1 : 7.8 : 3.3 for 100 nM PCB 11, 1 : 8.5 : 2.3 for 1 μ M PCB 11, and 1 : 5.0 : 1.2 for 10 μ M PCB 11 in a primary cortical cell culture model.⁵³ Another study with primary rat hippocampal neurons reported a mass ratio of PCB 136 between cells and media of 1 : 14.²⁰

Modeling the partitioning of PCBs in the HepG2 cell culture system. Studies with cells in culture typically report only the nominal concentrations of a toxicant, such as PCBs, and not the fraction of the toxicant that partitions into the cells. Thus, it is challenging to extrapolate from concentrations used in *in vitro* studies to tissue levels from *in vivo* studies. The amount of the toxicant in cells depends on its free concentration in the aqueous cell culture medium and the cells; however, the experimental determinations of the free concentration of a toxicant are challenging. Several composition-based models have been developed to predict the partitioning of different chemicals in microsomal incubations²⁵ and cell culture models,²² with the goal of relating nominal concentrations to free concentrations. However, these models have not been used to estimate the free concentrations of PCBs *in vitro*.

We employed a four-phase, composition-based model to describe the equilibrium partitioning of PCBs between cells and medium (Fig. 2a). This model is based on several assumptions: First, both cell culture medium and cells contain four biological components (i.e., protein, storage lipid, membrane lipid, and water). Second, PCBs have reached a partition equilibrium between proteins and water and between lipids and water. Third, the sorptive fractions (proteins, lipids, etc.) in medium change only insignificantly during the incubation. We used this model to predict

the free concentrations of the PCBs from both the initial amount of PCBs added in cell culture (Eq. 3) and the measured amount of PCBs in the medium after harvesting (Eq. 4). We employed different permutations of published experimental values for the biological components in cell culture medium and HepG2 cells because these values can show considerable variability (Table S3). Both methods estimated similar free concentrations of PCBs (Fig. 2b). It is, therefore, possible to approximate the free concentration of PCBs in cell culture-based assays based on their nominal concentrations and published experimental values for the biological components in the cell culture medium and the cells (Table S4).

***In vitro* to *in vivo* extrapolation.** We used the free PCB concentrations from our *in vitro* predictions, determined with Eq. 3, to extrapolate from the nominal PCB concentrations to PCB tissue concentrations with a published IVIVE model.²³ Based on this model, the PCB tissue levels equivalent to the *in vitro* concentrations (0.25 μ M) were 500 ± 60 , 490 ± 70 , 560 ± 80 and 580 ± 80 ng/g plasma and $6,200\pm800$, $6,100\pm800$, $7,200\pm1,000$ and $7,700\pm1,100$ ng/g liver wet weight for PCB 91, PCB 95, PCB 132 and PCB 136 *in vivo*, respectively (Fig. 3a). Furthermore, IVIVE coefficients, defined as the ratio of the PCB level *in vivo* (i.e., plasma or liver levels as ng/g wet weight) over the nominal concentration (in μ M) in the cell culture experiments, were calculated. The IVIVE coefficients were $2,000\pm300$, $2,000\pm300$, $2,200\pm300$ and $2,300\pm300$ for plasma and $25,000\pm3,200$, $24,000\pm3,100$, $29,000\pm4,000$ and $31,000\pm4,300$ for liver for PCB 91, PCB 95, PCB 132 and PCB 136, respectively (Table 1). These plasma IVIVE coefficients demonstrate that blood PCB levels are a poor rationale for the selection of nominal concentration for cell culture-based toxicity studies.

The IVIVE model also allowed us to estimate nominal concentrations for cell culture experiments that are equivalent to the PCB tissue levels observed *in vivo*. For example, liver

tissues levels of 1,800 ng/g for PCB 91, 1,200 ng/g for PCB 95 and 410 ng/g for PCB 136 observed in mice exposed orally to racemic PCBs⁵⁴⁻⁵⁶ correspond to nominal concentrations of 73 nM PCB 91, 49 nM PCB 95 and 13 nM PCB 136 in studies in HepG2 cells. Based on these estimations, the micromolar PCB concentrations employed in our study (0.25 μ M) are 4 to 14-times higher than the equivalent levels of the *in vivo* observations, even though micromolar concentrations are commonly used in *in vitro* studies.^{47,48} The model also enabled us to predict IVIVE extrapolation coefficients for all 209 PCBs for the experimental conditions employed in the present study (Fig. 3b). As expected, the extrapolation coefficients increased with an increasing degree of chlorination for plasma and liver. Relevant experimental parameters (e.g., cell number, medium volume, medium composition, etc.) are readily available from the published literature or can be determined experimentally. Thus, it is relatively easy to calculate similar extrapolation coefficients for other experimental systems using the spreadsheet provided in the Supporting Information.

Atropselective partitioning of PCBs in the HepG2 cell culture system. The PCB congeners investigated in this project bind atropselectively to cytochrome P450 enzymes⁴⁰ and undergo atropselective metabolism in the liver.^{37,55,56} Although this has not been studied previously, it is likely that PCBs interact enantioselectively with serum proteins, such as albumin. Therefore, we also assessed the atropselective partitioning of PCBs in our cell culture model.

Significant atropisomeric enrichment was detected in media, cells, and dishes for the four PCB congeners (Figs. 4&5). The atropisomer eluting first on a CD column (E_1) was significantly enriched in both cells and dishes for PCB 91 (i.e., (-)-PCB 91,⁵⁷; EF values of 0.77 for cells and 0.68 for dishes), PCB 132 (i.e., (-)-PCB 132⁵⁸; EF values of 0.69 for cells and 0.63 for dishes), and PCB 136 (i.e., (-)-PCB 136⁵⁸; EF values of 0.55 for cells and 0.68 for dishes). A slight

enrichment of E₁-PCB 95 (i.e., aR- or (-)-PCB 95⁵⁹) was observed, with EF values of 0.55 for cells and 0.53 for dishes.

The E₂-atropisomers of PCB 91, PCB 132 and PCB 136 were enriched in the cell culture medium, with EF values of 0.41, 0.44, and 0.47, respectively (Figs. 4&5). The PCB 95 residue was near racemic in the cell culture media samples, possibly because its high concentrations masked the atropisomeric enrichment. In parallel experiments, chiral analysis of samples from cell-free incubations revealed near-racemic chiral signatures in both dish and media samples (Fig. S4). These findings suggest that chiral PCBs enantioselectively partition between medium and cells in the HepG2 cell culture system in the absence of detectable PCB metabolism. Because we did not observe an atropselective partitioning in cell-free incubations, the atropisomeric enrichment appears to be driven by the selective partitioning of PCB atropisomers into the HepG2 cells.

Metabolism studies with human liver microsome showed a depletion of (+)-PCB 91,⁴² (+)-PCB 95³⁴ and (-)-PCB 132,⁶⁰ whereas (+)-PCB 91, (+)-PCB 95 and (+)-PCB 132 were enriched in HepG2 cells. These observations suggest that the enantioselective partitioning of PCBs in biological systems is determined by the complex biological components of cells and tissues. In contrast, only a small portion of enzymes (i.e., the active site of cytochrome P450 enzymes) is responsible for the subsequent atropselective metabolism of PCBs observed in *in vitro* metabolism studies.^{34, 40, 42, 60} Consistent with this interpretation, we have demonstrated that the binding of PCB 136 atropisomers to rat cytochrome P450 enzymes¹⁸ does not predict the atropselective metabolism of racemic PCB 136 by rat liver microsomes.³³

The results for the enantioselective analyses demonstrate that *in vitro* metabolism and toxicity studies with chiral compounds, including PCBs, should take their enantioselective partitioning

into account. Moreover, current composition-based models can not accurately describe the partitioning of chiral compounds in biological systems because they used the same chemical descriptors for the enantiomers; however, these models can be modified to incorporate enantioselective interactions with proteins (e.g., albumin or cytochrome P450 enzymes) and enantioselective metabolism.

CONFLICT OF INTEREST STATEMENT

The authors declare no competing financial interest.

FUNDING SOURCES

This work was supported by grants ES027169, ES013661, and ES005605 from the National Institute of Environmental Health Sciences, National Institutes of Health. The content is solely the responsibility of the authors and does not necessarily represent the official views of the National Institute of Environmental Health Sciences or the National Institutes of Health.

ACKNOWLEDGMENTS

Thanks to Dr. Lynn Teesch and Mr. Vic Parcell (High-Resolution Mass Spectrometry Facility, University of Iowa) for help with the chemical analysis, and Drs. Ram Dhakal, Xueshu Li, Xianran He, and Wenjin Xu (University of Iowa) for the synthesis of PCB metabolite standards.

372 SUPPORTING INFORMATION

373 Details regarding the deconjugation procedures, untargeted analysis, mathematic details of
374 the partitioning models, chemical standards, enantiomeric fractions, quality assurance/quality
375 control data, biological compositions, cytotoxicity data, overall extraction workflow, sorptive
376 capacities of chemicals, and partitioning of PCBs in cell-free incubations. This material is
377 available free of charge via the Internet at <http://pubs.acs.org>.

REFERENCES

1. Fiedler, H.; Abad, E.; van Bavel, B.; de Boer, J.; Bogdal, C.; Malisch, R. The need for capacity building and first results for the Stockholm Convention Global Monitoring Plan. *Trac-Trend Anal Chem* **2013**, *46*, 72-84.
2. PCBs-overview.
<http://www.pops.int/Implementation/IndustrialPOPs/PCB/Overview/tabid/273/Default.aspx>
(Accessed on Mar 19, 2020),
3. Hu, D.F.; Hornbuckle, K.C. Inadvertent polychlorinated biphenyls in commercial paint pigments. *Environ Sci Technol* **2010**, *44*, 2822-2827.
4. Herkert, N.J.; Jahnke, J.C.; Hornbuckle, K.C. Emissions of tetrachlorobiphenyls (PCBs 47, 51, and 68) from polymer resin on kitchen cabinets as a non-aroclor source to residential air. *Environ Sci Technol* **2018**, *52*, 5154-5160.
5. Anezaki, K.; Kannan, N.; Nakano, T. Polychlorinated biphenyl contamination of paints containing polycyclic- and Naphthol AS-type pigments. *Environ Sci Pollut Res* **2015**, *22*, 14478-14488.
6. Marek, R.F.; Thome, P.S.; Herkert, N.J.; Awad, A.M.; Hornbuckle, K.C. Airborne PCBs and OH-PCBs inside and outside urban and rural US schools. *Environ Sci Technol* **2017**, *51*, 7853-7860.
7. Gabrio, T.; Piechotowski, I.; Wallenhorst, T.; Klett, M.; Cott, L.; Friebel, P.; Link, B.; Schwenk, M. PCB-blood levels in teachers, working in PCB-contaminated schools. *Chemosphere* **2000**, *40*, 1055-1062.
8. Banyiova, K.; Cerna, M.; Mikes, O.; Komprdova, K.; Sharma, A.; Gyalpo, T.; Cupr, P.; Scheringer, M. Long-term time trends in human intake of POPs in the Czech Republic indicate a need for continuous monitoring. *Environ Int* **2017**, *108*, 1-10.
9. Raffetti, E.; Speziani, F.; Donato, F.; Leonardi, L.; Orizio, G.; Scarcella, C.; Apostoli, P.; Magoni, M. Temporal trends of polychlorinated biphenyls serum levels in subjects living in a highly polluted area from 2003 to 2015: a follow-up study. *Int J Hyg Envir Heal* **2017**, *220*, 461-467.

- 403 10. Boitsov, S.; Grosvik, B.E.; Nesje, G.; Malde, K.; Klungsoyr, J. Levels and temporal trends of
404 persistent organic pollutants (POPs) in Atlantic cod (*Gadus morhua*) and haddock
405 (*Melanogrammus aeglefinus*) from the southern Barents Sea. *Environ Res* **2019**, *172*, 89-97.
- 406 11. ATSDR Toxic Substances Portal - Polychlorinated Biphenyls (PCBs).
407 <https://www.atsdr.cdc.gov/ToxProfiles/tp.asp?id=142&tid=26> (Accessed on Mar 19, 2020),
- 408 12. Pessah, I.N.; Cherednichenko, G.; Lein, P.J. Minding the calcium store: Ryanodine receptor
409 activation as a convergent mechanism of PCB toxicity. *Pharmacol Therapeut* **2010**, *125*, 260-285.
- 410 13. Lehmler, H.J.; Harrad, S.J.; Huhnerfuss, H.; Kania-Korwel, I.; Lee, C.M.; Lu, Z.; Wong, C.S.
411 Chiral polychlorinated biphenyl transport, metabolism, and distribution: A review. *Environ Sci*
412 *Technol* **2010**, *44*, 2757-2766.
- 413 14. Kania-Korwel, I.; Lehmler, H.J. Chiral polychlorinated biphenyls: absorption, metabolism and
414 excretion-a review. *Environ Sci Pollut Res* **2016**, *23*, 2042-2057.
- 415 15. Konishi, Y.; Kakimoto, K.; Nagayoshi, H.; Nakano, T. Trends in the enantiomeric composition of
416 polychlorinated biphenyl atropisomers in human breast milk. *Environ Sci Pollut R* **2016**, *23*, 2027-
417 2032.
- 418 16. Rodman, L.E.; Shedlofsky, S.I.; Swim, A.T.; Robertson, L.W. Effects of polychlorinated-biphenyls
419 on cytochrome-P450 induction in the chick-embryo hepatocyte culture. *Arch Biochem Biophys*
420 **1989**, *275*, 252-262.
- 421 17. Puttmann, M.; Mannschreck, A.; Oesch, F.; Robertson, L. Chiral effects in the induction of drug-
422 metabolizing-enzymes using synthetic atropisomers of polychlorinated-Biphenyls (PCBs).
423 *Biochem Pharmacol* **1989**, *38*, 1345-1352.
- 424 18. Kania-Korwel, I.; Hrycay, E.G.; Bandiera, S.M.; Lehmler, H.J. 2,2',3,3',6,6'-hexachlorobiphenyl
425 (PCB 136) atropisomers interact enantioselectively with hepatic microsomal cytochrome P450
426 enzymes. *Chem Res Toxicol* **2008**, *21*, 1295-1303.

19. Pessah, I.N.; Lehmler, H.J.; Robertson, L.W.; Perez, C.F.; Cabrales, E.; Bose, D.D.; Feng, W. Enantiomeric specificity of (-)-2,2',3,3',6,6'-hexachlorobiphenyl toward ryanodine receptor types 1 and 2. *Chem Res Toxicol* **2009**, *22*, 201-207.
20. Yang, D.R.; Kania-Korwel, I.; Ghogha, A.; Chen, H.; Stamou, M.; Bose, D.D.; Pessah, I.N.; Lehmler, H.J.; Lein, P.J. PCB 136 atropselectively alters morphometric and functional parameters of neuronal connectivity in cultured rat hippocampal neurons via ryanodine receptor-dependent mechanisms. *Toxicol Sci* **2014**, *138*, 379-392.
21. Feng, W.; Zheng, J.; Robin, G.; Dong, Y.; Ichikawa, M.; Inoue, Y.; Mori, T.; Nakano, T.; Pessah, I.N. Enantioselectivity of 2,2',3,5',6-pentachlorobiphenyl (PCB 95) atropisomers toward ryanodine receptors (RyRs) and their influences on hippocampal neuronal networks. *Environ Sci Technol* **2017**, *51*, 14406-14416.
22. Fischer, F.C.; Henneberger, L.; Konig, M.; Bittermann, K.; Linden, L.; Goss, K.U.; Escher, B.I. Modeling exposure in the Tox21 in vitro bioassays. *Chem Res Toxicol* **2017**, *30*, 1197-1208.
23. Gulden, M.; Seibert, H. In vitro in vivo extrapolation: estimation of human serum concentrations of chemicals equivalent to cytotoxic concentrations in vitro (vol 189, pg 211, 2003). *Toxicology* **2003**, *192*, 265-265.
24. Armitage, J.M.; Wania, F.; Arnot, J.A. Application of mass balance models and the chemical activity concept to facilitate the use of in vitro toxicity data for risk assessment. *Environ Sci Technol* **2014**, *48*, 9770-9779.
25. Poulin, P.; Haddad, S. Microsome composition-based model as a mechanistic tool to predict nonspecific binding of drugs in liver microsomes. *J Pharm Sci-US* **2011**, *100*, 4501-4517.
26. Poulin, P.; Haddad, S. Hepatocyte composition-based model as a mechanistic tool for predicting the cell suspension: Aqueous phase partition coefficient of drugs in in vitro metabolic studies. *J Pharm Sci-US* **2013**, *102*, 2806-2818.

27. Endo, S.; Brown, T.N.; Goss, K.U. General model for estimating partition coefficients to organisms and their tissues using the biological compositions and polyparameter linear free energy relationships. *Environ Sci Technol* **2013**, *47*, 6630-6639.
28. van Noort, P.C.M.; Haftka, J.J.H.; Parsons, J.R. Updated Abraham solvation parameters for polychlorinated biphenyls. *Environ Sci Technol* **2010**, *44*, 7037-7042.
29. Dhakal, K.; He, X.R.; Lehmler, H.J.; Teesch, L.M.; Duffel, M.W.; Robertson, L.W. Identification of sulfated metabolites of 4-chlorobiphenyl (PCB3) in the serum and urine of male rats. *Chem Res Toxicol* **2012**, *25*, 2796-2804.
30. Shaikh, N.S.; Parkin, S.; Lehmler, H.J. The ullmann coupling reaction: A new approach to tetraarylstannanes. *Organometallics* **2006**, *25*, 4207-4214.
31. Joshi, S.N.; Vyas, S.M.; Duffel, M.W.; Parkin, S.; Lehmler, H.J. Synthesis of sterically hindered polychlorinated biphenyl derivatives. *Synthesis-Stuttgart* **2011**, 1045-1054.
32. Kania-Korwel, I.; Duffel, M.W.; Lehmler, H.J. Gas chromatographic analysis with chiral cyclodextrin phases reveals the enantioselective formation of hydroxylated polychlorinated biphenyls by rat liver microsomes. *Environ Sci Technol* **2011**, *45*, 9590-9596.
33. Wu, X.A.; Pramanik, A.; Duffel, M.W.; Hrycay, E.G.; Bandiera, S.M.; Lehmler, H.J.; Kania-Korwel, I. 2,2',3,3',6,6'-Hexachlorobiphenyl (PCB 136) Is Enantioselectively Oxidized to Hydroxylated Metabolites by Rat Liver Microsomes. *Chem Res Toxicol* **2011**, *24*, 2249-2257.
34. Uwimana, E.; Li, X.S.; Lehmler, H.J. 2,2',3,5',6-Pentachlorobiphenyl (PCB 95) is atropselectively metabolized to para-hydroxylated metabolites by human liver microsomes. *Chem Res Toxicol* **2016**, *29*, 2108-2110.
35. Kania-Korwel, I.; Zhao, H.X.; Norstrom, K.; Li, X.S.; Hornbuckle, K.C.; Lehmler, H.J. Simultaneous extraction and clean-up of polychlorinated biphenyls and their metabolites from small tissue samples using pressurized liquid extraction. *J Chromatogr A* **2008**, *1214*, 37-46.
36. Kania-Korwel, I.; Hornbuckle, K.C.; Peck, A.; Ludewig, G.; Robertson, L.W.; Sulkowski, W.W.; Espandiari, P.; Gairola, C.G.; Lehmler, H.J. Congener-specific tissue distribution of aroclor 1254

and a highly chlorinated environmental PCB mixture in rats. *Environ Sci Technol* **2005**, *39*, 3513-3520.

37. Kania-Korwel, I.; Shaikh, N.S.; Hornbuckle, K.C.; Robertson, L.W.; Lehmler, H.J. Enantioselective disposition of PCB 136 (2,2',3,3',6,6'-hexachlorobiphenyl) in C57BL/6 mice after oral and intraperitoneal administration. *Chirality* **2007**, *19*, 56-66.

38. Commission, E. Commission Decision EC 2002/657 of 12 August 2002 implementing Council Directive 96/23/EC concerning the performance of analytical methods and the interpretation of results. *Off. J. Eur. Communities: Legis* **2002**, *221*.

39. Uwimana, E.; Maiers, A.; Li, X.S.; Lehmler, H.J. Microsomal metabolism of prochiral polychlorinated biphenyls results in the enantioselective formation of chiral metabolites. *Environ Sci Technol* **2017**, *51*, 1820-1829.

40. Uwimana, E.; Ruiz, P.; Li, X.S.; Lehmler, H.J. Human CYP2A6, CYP2B6, AND CYP2E1 atropselectively metabolize polychlorinated biphenyls to hydroxylated metabolites. *Environ Sci Technol* **2019**, *53*, 2114-2123.

41. Kania-Korwel, I.; El-Komy, M.H.M.E.; Veng-Pedersen, P.; Lehmler, H.J. Clearance of polychlorinated biphenyl atropisomers is enantioselective in female C57BL/6 mice. *Environ Sci Technol* **2010**, *44*, 2828-2835.

42. Uwimana, E.; Li, X.S.; Lehmler, H.J. Human liver microsomes atropselectively metabolize 2,2',3,4',6-pentachlorobiphenyl (PCB 91) to a 1,2-shift product as the major metabolite. *Environ Sci Technol* **2018**, *52*, 6000-6008.

43. Geisler, A.; Endo, S.; Goss, K.U. Partitioning of organic chemicals to storage lipids: Elucidating the dependence on fatty acid composition and temperature. *Environ Sci Technol* **2012**, *46*, 9519-9524.

44. Endo, S.; Escher, B.I.; Goss, K.U. Capacities of membrane lipids to accumulate neutral organic chemicals. *Environ Sci Technol* **2011**, *45*, 5912-5921.

- 502 45. Zhu, X.P.; Yan, H.M.; Xia, M.F.; Chang, X.X.; Xu, X.; Wang, L.; Sun, X.Y.; Lu, Y.; Bian, H.; Li,
503 X.Y.; Gao, X. Metformin attenuates triglyceride accumulation in HepG2 cells through decreasing
504 stearyl-coenzyme A desaturase 1 expression. *Lipids Health Dis* **2018**, *17*.
- 505 46. Cheever, M.; Master, A.; Versteegen, R.J. A method for differentiating fetal bovine serum from
506 newborn calf serum. *BioProcessing Journal* **2017**, *16*.
- 507 47. Huang, M.; Zhang, L.; Mesaros, C.; Zhang, S.H.; Blaha, M.A.; Blair, I.A.; Penning, T.M.
508 Metabolism of a representative oxygenated polycyclic aromatic hydrocarbon (PAH) phenanthrene-
509 9,10-quinone in human hepatoma (HepG2) cells. *Chem Res Toxicol* **2014**, *27*, 852-863.
- 510 48. Huang, M.; Zhang, L.; Mesaros, C.; Hackfeld, L.C.; Hodge, R.P.; Bair, I.A.; Penning, T.M.
511 Metabolism of an alkylated polycyclic aromatic hydrocarbon 5-methylchrysene in human
512 hepatoma (HepG2) cells. *Chem Res Toxicol* **2015**, *28*, 2045-2058.
- 513 49. Zhang, H.N.; Shao, X.J.; Zhao, H.Z.; Li, X.N.; Wei, J.T.; Yang, C.X.; Caio, Z.W. Integration of
514 metabolomics and lipidomics reveals metabolic mechanisms of triclosan-induced toxicity in human
515 hepatocytes. *Environ Sci Technol* **2019**, *53*, 5406-5415.
- 516 50. Hart, S.N.; Li, Y.; Nakamoto, K.; Subileau, E.A.; Steen, D.; Zhong, X.B. A comparison of whole
517 genome gene expression profiles of HepaRG cells and HepG2 cells to primary human hepatocytes
518 and human liver tissues. *Drug Metab Dispos* **2010**, *38*, 988-994.
- 519 51. Grimm, F.A.; Hu, D.F.; Kania-Korwel, I.; Lehmler, H.J.; Ludewig, G.; Hornbuckle, K.C.; Duffel,
520 M.W.; Bergman, A.; Robertson, L.W. Metabolism and metabolites of polychlorinated biphenyls.
521 *Crit Rev Toxicol* **2015**, *45*, 245-272.
- 522 52. Rodriguez, E.A.; Li, X.; Lehmler, H.J.; Robertson, L.W.; Duffel, M.W. Sulfation of lower
523 chlorinated polychlorinated biphenyls increases their affinity for the major drug-binding sites of
524 human serum albumin. *Environ Sci Technol* **2016**, *50*, 5320-5327.
- 525 53. Sethi, S.; Keil, K.P.; Chen, H.; Hayakawa, K.; Li, X.; Lin, Y.; Lehmler, H.J.; Puschner, B.; Lein,
526 P.J. Detection of 3,3'-dichlorobiphenyl in human maternal plasma and its effects on axonal and
527 dendritic growth in primary rat neurons. *Toxicol Sci* **2017**, *158*, 401-411.

54. Wu, X.N.; Barnhart, C.; Lein, P.J.; Lehmler, H.J. Hepatic metabolism affects the atropselective disposition of 2,2',3,3',6,6'-hexachlorobiphenyl (PCB 136) in mice. *Environ Sci Technol* **2015**, *49*, 616-625.
55. Kania-Korwel, I.; Barnhart, C.D.; Stamou, M.; Truong, K.M.; El-Komy, M.H.M.E.; Lein, P.J.; Veng-Pedersen, P.; Lehmler, H.J. 2,2',3,5',6-Pentachlorobiphenyl (PCB 95) and its hydroxylated metabolites are enantiomerically enriched in female mice. *Environ Sci Technol* **2012**, *46*, 11393-11401.
56. Wu, X.; Zhai, G.; Schnoor, J.L.; Lehmler, H.J. Atropselective disposition of 2,2',3,4',6-pentachlorobiphenyl (PCB 91) and identification of its metabolites in mice with liver-specific deletion of cytochrome P450 reductase. *Chem Res Toxicol* **2019**.
57. He, Z.Y.; Wang, Y.H.; Zhang, Y.W.; Cheng, H.Y.; Liu, X.W. Stereoselective bioaccumulation of chiral PCB 91 in earthworm and its metabolomic and lipidomic responses. *Environ Pollut* **2018**, *238*, 421-430.
58. Haglund, P.; Wiberg, K. Determination of the gas chromatographic elution sequences of the (+)- and (-)-enantiomers of stable atropisomeric PCBs on Chirasil-Dex. *Hrc-J High Res Chrom* **1996**, *19*, 373-376.
59. Nagayoshi, H.; Kakimoto, K.; Konishi, Y.; Kajimura, K.; Nakano, T. Determination of the human cytochrome P450 monooxygenase catalyzing the enantioselective oxidation of 2,2',3,5',6-pentachlorobiphenyl (PCB 95) and 2,2',3,4,4',5',6-heptachlorobiphenyl (PCB 183). *Environ Sci Pollut Res* **2018**, *25*, 16420-16426.
60. Uwimana, E.; Cagle, B.; Yeung, C.; Li, X.S.; Patterson, E.V.; Doorn, J.A.; Lehmler, H.J. Atropselective oxidation of 2,2',3,3',4,6'-hexachlorobiphenyl (PCB 132) to hydroxylated metabolites by human liver microsomes and its implications for PCB 132 neurotoxicity. *Toxicol Sci* **2019**, *171*, 406-420.

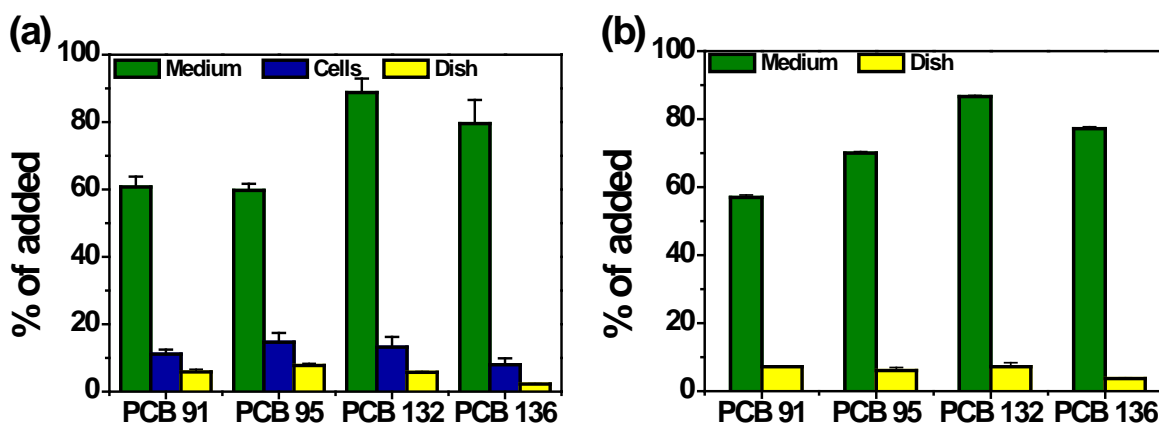
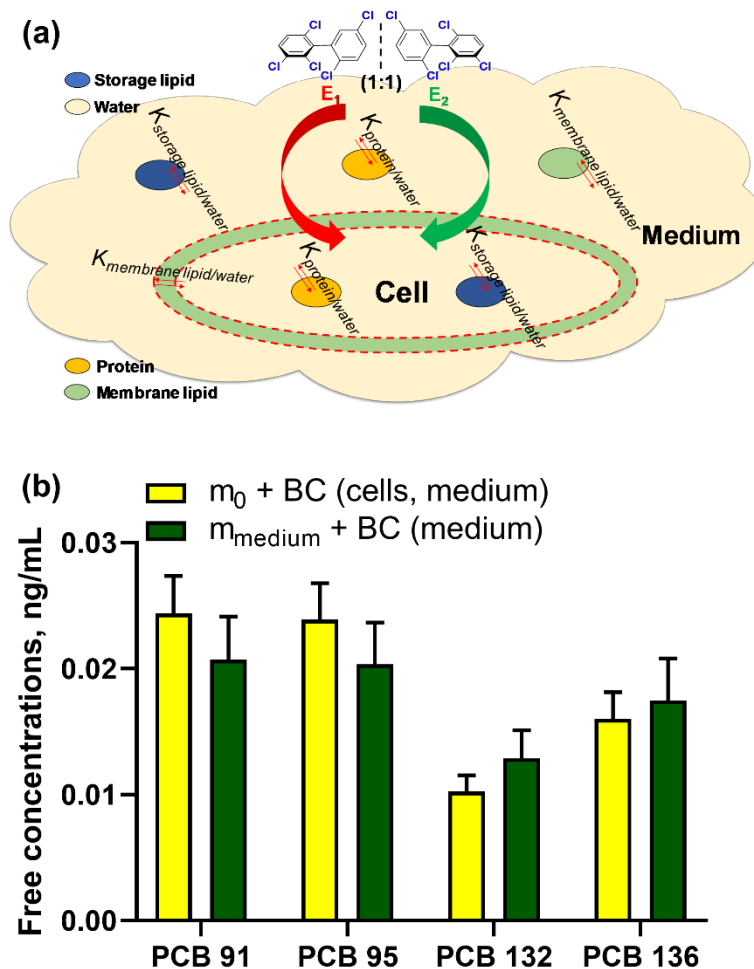


Fig. 1. PCB 91, PCB 95, PCB 132, and PCB 136 were primarily present in the cell culture medium from experiments (a) with or (b) without HepG2 cells. Only a small percentage of the PCBs were recovered from the cell pellet (7.9 to 14.7 %) or the cell culture dish (2.2 to 7.8 %). HepG2 cells (6×10^6 /well) were seeded into 6-well plates with complete MEM medium (3 mL) per well and allowed to attach for 48 h. Cells were exposed for 72 h to the individual PCB congeners (0.25 μ M; 0.1 % DMSO) in exposure medium (3 mL) with 10 % FBS. Controls were exposed to 0.1 % DMSO in the exposure medium. After the incubation, the media, cell pellets, and cell culture dishes were collected, and PCB levels were determined as described in the Experimental Section.

561



562

Fig. 2. (a) A four-phase, composition-based model was used to describe the distributions of PCB 91, PCB 95, PCB 132, and PCB 136 between cell culture medium and cells. (b) Similar free concentrations were estimated with the models using either the initial mass of PCBs (m_0) coupled with biological components (BC) in cells and medium or the measured mass of PCBs (m_{medium}) in medium coupled with the BC in the medium. Eqs. (3) and (4) were used for the predictions, respectively. The free concentrations are presented as the average \pm standard deviations of the results obtained with different values for the quantities of biological components in cell culture system (for additional information, see Table S4).

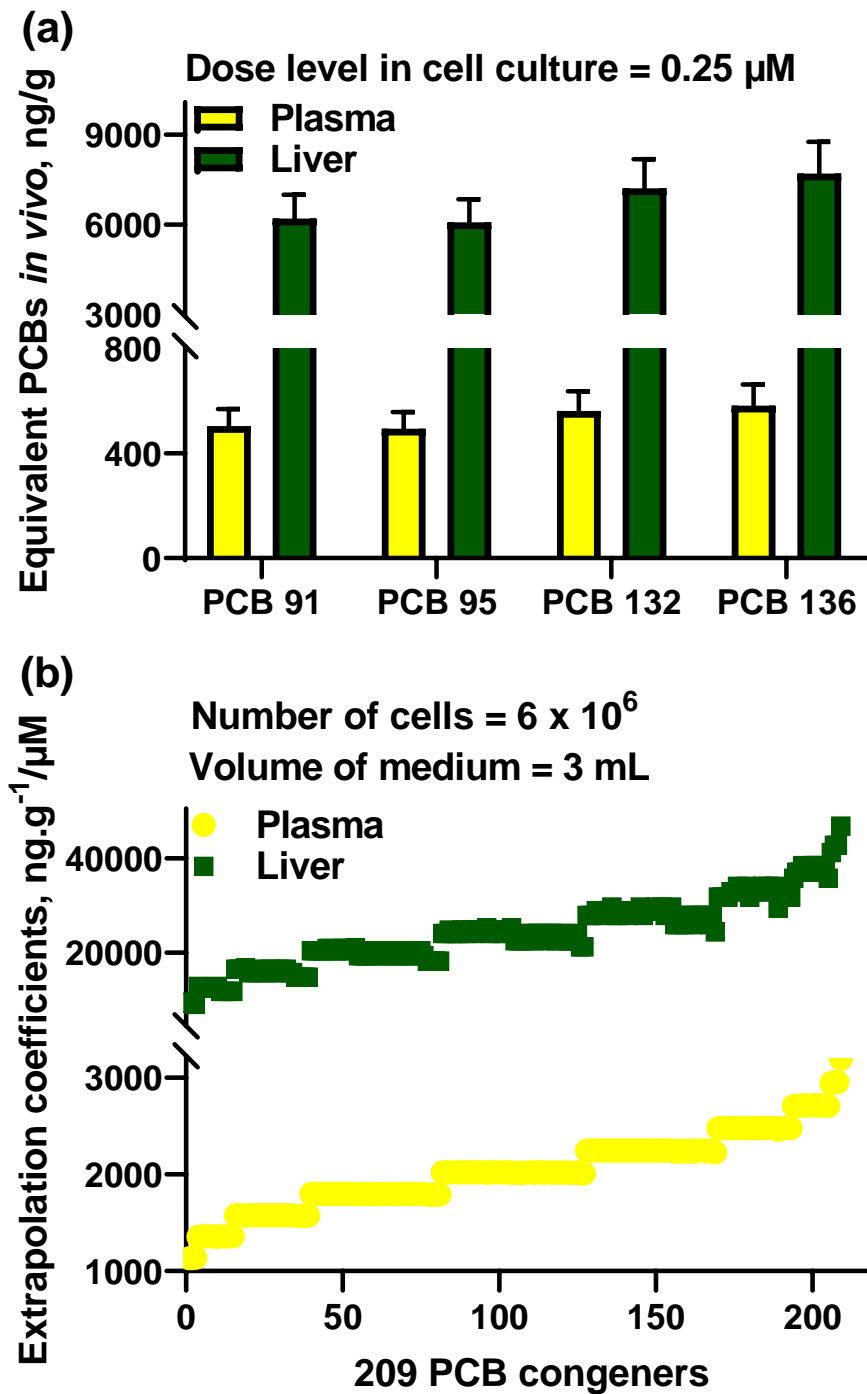


Fig. 3. The *in vitro-in vivo* extrapolation predicted (a) the equivalent *in vivo* plasma and liver levels of the four PCB congeners studied (PCB 91, PCB 95, PCB 132, and PCB 136) corresponding to 0.25 μM dose level in cell culture and (b) the trend of plasma and liver extrapolation coefficients for 209 PCB congeners under the cell culture conditions employed in

576 this study. Eqs. (5) and (6) were used for the predictions. The equivalent tissue levels of PCB 91,
577 PCB 95, PCB 132, and PCB 136 are presented as the average \pm standard deviations of the results
578 obtained with different values for the quantities of biological components in the cell culture
579 system (for additional information, see Table S4). The extrapolation coefficients of the 209 PCB
580 congeners were given as the average value obtained from various permutations using the data
581 sources listed in Table S4. The solvation parameters of PCBs and the quantities of the biological
582 components in *in vivo* plasma and liver used for the predictions were obtained from the
583 literature.^{27,28}

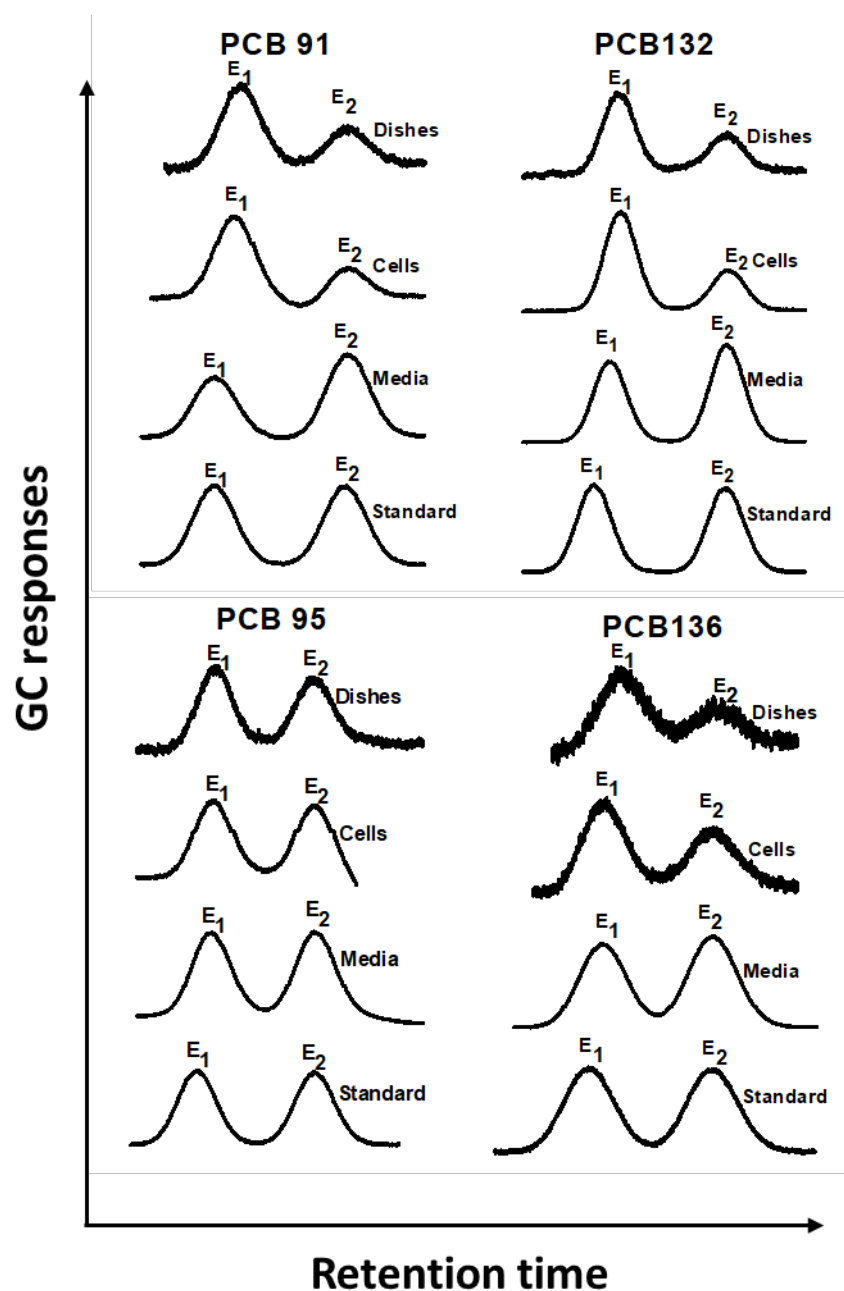


Fig. 4. Representative chromatograms show an atropisomeric enrichment in extracts from cell culture media, cell pellet and cell culture dishes after incubation with racemic (a) PCB 91, (b) PCB 95, (c) PCB 132 and (d) PCB 136. The atropisomeric enrichment of these parent PCBs occurs in the absence of any detectable metabolism. The racemic PCB standards are shown for comparison. HepG2 cells (6×10^6 /well) were exposed for 72 h to the individual, racemic PCB congeners (10

590 μM ; 0.1 % DMSO) in exposure medium (3 mL) with 10 % FBS. After the incubation, the media,
591 cells and cell culture dishes were collected, and enantioselective analyses were performed by GC-
592 μECD using a CD capillary column as described in the Experimental Section. E_1 and E_2 are the
593 atropisomers eluting first and second on the CD capillary column.

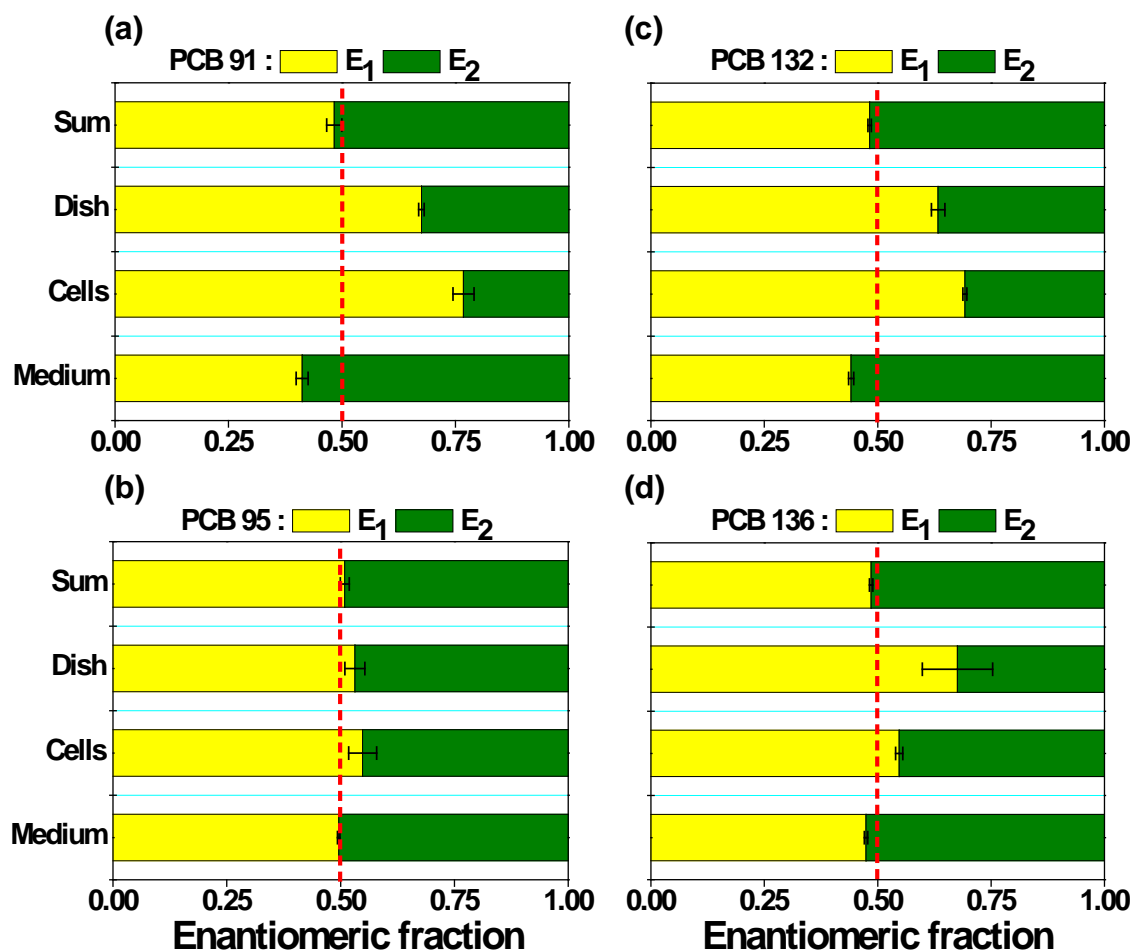


Fig. 5. The direction of the atropisomeric enrichment of (a) PCB 91, (b) PCB 95, (c) PCB 132 and (d) PCB 136 in HepG2 cells and cell culture dishes is opposite to the atropisomeric enrichment observed in the cell culture media. HepG2 cells (6×10^6 /well) were exposed for 72 h to the individual, racemic PCB congeners ($10 \mu\text{M}$; 0.1 % DMSO) in exposure medium (3 mL) with 10 % FBS. After the incubation, the media, cells and cell culture dishes were collected, and enantioselective analyses were performed by GC- μ ECD using a CD capillary column as described in the Experimental Section. The dotted line indicates the EF value of the respective racemic PCB congener.

SUPPORTING INFORMATION

Enantioselective Partitioning of Polychlorinated Biphenyls in a HepG2 Cell Culture System: Experimental and Modeling Results

Chun-Yun Zhang¹, Susanne Flor¹, Gabriele Ludewig¹, Hans-Joachim Lehmler^{1,*}

¹Department of Occupational and Environmental Health, The University of Iowa,

Iowa City, Iowa 52242, United States

Corresponding Author:

Dr. Hans-Joachim Lehmler

The University of Iowa

Department of Occupational and Environmental Health

University of Iowa Research Park, B164 MTF

Iowa City, IA 52242-5000

Phone: (319) 335-4981

Fax: (319) 335-4290

e-mail: hans-joachim-lehmler@uiowa.edu

Number of pages: 20

Number of tables: 4

Number of figures: 4

Table of Content

Extraction of medium samples and subsequent deconjugation experiments	S3
Extraction of medium samples for untargeted analyses	S3
Ultra-Performance Liquid Chromatography-Quadrupole Time-of-flight Mass Spectrometric (LC-QToF-MS) analysis	S4
Prediction of the free concentrations of PCBs in the cell culture system	S4
<i>In vitro-in vivo</i> extrapolation (IVIVE)	S6
Table S1. Summary of the chemical structure, the abbreviation and the source of available hydroxylated or methoxylated standards	S8
Table S2. Comparison of the enantiomeric fractions (EFs) of PCBs in the HepG2 cell culture system determined with different enantioselective columns	S11
Table S3. Quality assurance/quality control (QA/QC) data for the quantitative and chiral analysis of the PCBs	S13
Table S4. The permutations of the system descriptors in HepG2 cell culture system used for the model calculations	S14
Fig. S1. The cytotoxicity of PCBs (PCB 91, PCB 95, PCB 132, and PCB 136) toward HepG2 cells	S15
Fig. S2. Overall extraction workflow of PCBs and their metabolites from the cell culture media, cell pellets and dishes	S16
Fig. S3. The differences in the sorptive capacities (as partition coefficients) of chemicals between storage lipids and membrane lipids	S17
Fig. S4. The partitioning of PCB 91, PCB 95, PCB 132 and PCB 136 in a cell-free culture system	S18
References	S19

Extraction of medium samples and subsequent deconjugation experiments. PCBs and their metabolites were extracted from the medium of HepG2 cells exposed for 72 h to PCBs (1 μ M) with hexane/MTBE (see Manuscript for additional details regarding the cell culture experiments). The remaining aqueous phase was spiked with 3-F,4'-PCB 3 sulfate (100 ng in methanol), followed by extraction with ethyl acetate (4 mL and 3 mL). Earlier studies have shown that ethyl acetate is an excellent solvent for the extraction of PCB metabolites, including their conjugates, from aqueous media.¹ 3-F,4'-PCB 3 sulfate (100 ng in methanol) was also added as surrogate recovery standard to blank solvent (buffer) samples. The F-tagged sulfate standard was used to assess the efficiency of the deconjugation of PCB sulfates and the derivatization of the resulting OH-PCBs with diazomethane. The combined organic phase was evaporated to dryness and reconstituted in sodium acetate buffer (4 mL, pH=5). After the addition of sulfatase (type H-2 from *Helix pomatia*, 50 μ L, \geq 2,000 units/mL), each sample was incubated at 37 °C for 16 hours to deconjugate PCB conjugates to the corresponding OH-PCB metabolites. All samples were extracted, derivatized, and analyzed by GC-ECD as described in the Experimental Section for medium samples. No methoxylated PCBs metabolites were detected in any sample, except for the F-tagged OH-PCB derivative.

Extraction of medium samples from PCB exposed HepG2 cell culture for untargeted analyses. Medium samples from HepG2 cells exposed to PCBs (1 μ M) for 72 h were extracted for untargeted analysis (Fig. S2). Briefly, the samples were spiked with 3-F,4'-OH PCB 3 and 3-F,4'-PCB 3 sulfate (100 ng each in methanol) as surrogate recovery standards to monitor the performance of the extraction and the untargeted ultra-performance liquid chromatography-quadrupole time-of-flight mass spectrometric (LC-QToF-MS) analyses. Samples were extracted with acetonitrile (4 mL) after the addition of magnesium sulfate (1.2 g)

and sodium chloride (0.3 g). The aqueous phase was re-extracted with acetonitrile (3 mL). The combined organic phase was passed through a magnesium sulfate (2 g) column to remove water. The extract was evaporated to dryness under a gentle stream of nitrogen and reconstituted in acetonitrile : water (15:85, v/v). LC-QToF MS analysis was performed as described below.

Ultra-Performance Liquid Chromatography-Quadrupole Time-of-flight Mass

Spectrometric (LC-QToF-MS) analysis. The LC-QToF MS analysis was carried out on a Waters Acquity UPLC (Waters, Milford, MA, USA) coupled with a Waters Q-ToF Premier mass spectrometer in the High-Resolution Mass Spectrometry Facility of the University of Iowa (Iowa City, IA, USA). An Acquity BEH C-18 column (2.1 mm inner diameter, 100 mm length, 1.7 μ m particle size; Waters) was used for the chromatographic separation of potential PCB metabolites, with a flow rate of 0.2 mL/min. The mobile phase was (A) water with 0.04 % (v/v) triethylammonium and (B) acetonitrile. The solvent gradient (% (B)) was as follows: 0-1 min, 15%; 1-10 min, 15-95 %, 10-15 min, 95 %. The full scan was performed in the ESI⁻ mode with a mass-to-charge ratio (m/z) range from 75 to 800 Da at a rate of 0.2s/scan. Leucine enkephalin was infused (10 μ L/min) as the lock mass and analyzed separately in ESI⁻ mode. The sampling cone voltage was 30 V. The desolvation gas was operated at 350 °C at a flow rate of 650 L/h. The capillary voltage was 2.8 kV. Full scan raw data were screened for potential penta- or hexachlorinated PCB metabolites, including mono- and di-hydroxylated PCBs, PCB sulfates, PCB glucuronides, and PCB dihydrodiols and their conjugates.² No PCB metabolite was detected in any medium sample.

Prediction of the free concentrations of PCBs in the cell culture system. As shown in Fig. 2a, the PCBs are distributed between the different biological components (i.e., albumin

protein, storage lipid, membrane lipid, and water) in both medium and cells. The mass balance in the whole system (cell culture dish is excluded), medium and cells can be expressed as

$$m_0 = m_{medium} + m_{cell} \quad (S-1)$$

$$m_{medium} = C_{m,ap}V_{m,ap} + C_{m,sl}V_{m,sl} + C_{m,ml}V_{m,ml} + C_{m,w}V_{m,w} \quad (S-2)$$

and

$$m_{cell} = C_{c,ap}V_{c,ap} + C_{c,sl}V_{c,sl} + C_{c,ml}V_{c,ml} + C_{c,w}V_{c,w} \quad (S-3)$$

respectively. m_0 is the mass of PCBs initially added in the incubation. m_{medium} and m_{cell} are the amounts of PCBs present in the medium and in the cells, respectively. The m_0 values used for the model calculations in this study were corrected by subtracting the measured levels of PCBs in dishes (about 5.7 % at average). $C_{m,ap}$, $C_{m,sl}$, $C_{m,ml}$ and $C_{m,w}$ are the PCBs concentrations in the albumin protein, storage lipid, membrane lipid, and water in medium, respectively. $C_{c,ap}$, $C_{c,sl}$, $C_{c,ml}$ and $C_{c,w}$ are the PCBs concentrations in the albumin protein, storage lipid, membrane lipid, and water in cells, respectively. $V_{m,ap}$, $V_{m,sl}$, $V_{m,ml}$ and $V_{m,w}$ are the volumes of the protein, storage lipid, membrane lipid, and water in medium, respectively. $V_{c,ap}$, $V_{c,sl}$, $V_{c,ml}$ and $V_{c,w}$ are the volumes of the albumin protein, storage lipid, membrane lipid, and water in cells, respectively.

Assuming a partitioning equilibrium was reached in the system, the partition coefficients between albumin protein ($K_{ap,w}$), storage lipid ($K_{sl,w}$), membrane lipid ($K_{ml,w}$), and water can be expressed as:

$$K_{p,w} = \frac{C_{m,ap}}{C_{m,w}} = \frac{C_{c,ap}}{C_{c,w}}, \quad (S-4)$$

$$K_{sl,w} = \frac{C_{m,sl}}{C_{m,w}} = \frac{C_{c,sl}}{C_{c,w}}, \text{ and} \quad (S-5)$$

$$K_{ml,w} = \frac{C_{m,ml}}{C_{m,w}} = \frac{C_{c,ml}}{C_{c,w}} \quad (S-6)$$

Substituting Eqs. (S-4), (S-5) and (S-6) into Eqs (S-1) and (S-2) gives the following equations:

$$m_0 = C_{m,w}(K_{p,w}V_{m,p} + K_{sl,w}V_{m,sl} + K_{ml,w}V_{m,ml} + V_{m,w}) + C_{c,w}(K_{p,w}V_{c,p} + K_{sl,w}V_{c,sl} + K_{ml,w}V_{c,ml} + V_{c,w}) \quad (S-7)$$

and

$$m_{medium} = C_{m,w}(K_{p,w}V_{m,p} + K_{sl,w}V_{m,sl} + K_{ml,w}V_{m,ml} + V_{m,w}) \quad (S-8)$$

Assuming that free PCB concentrations (C_{free}) are equal in the medium ($C_{m,w}$) and cells ($C_{c,w}$) in the equilibrium state, i.e.,

$$C_{free} = C_{m,w} = C_{c,w} \quad (S-9)$$

Eq. (S-7) and (S-8) can be rearranged to calculate C_{free} as Eq. (3)

$$C_{free} = \frac{m_0}{K_{ap,w}(V_{m,ap} + V_{c,ap}) + K_{ml,w}(V_{m,ml} + V_{c,ml}) + K_{sl,w}(V_{m,sl} + V_{c,sl}) + V_{m,w} + V_{c,w}} \quad (S-10)$$

and as Eq. (4)

$$C_{free} = \frac{m_0}{K_{ap,w}V_{m,ap} + K_{ml,w}V_{m,ml} + K_{sl,w}V_{m,sl} + V_{m,w}} \quad (S-11)$$

In vitro-in vivo extrapolation (IVIVE). A composition-based model was used to describe the partitioning of the PCBs in tissues *in vivo* for the IVIVE. In this model, the biological components in tissues (including plasma) were assumed to be albumin proteins, muscle proteins, storage lipids, membrane lipids, and water.³ The mass balance of the PCBs in tissues can be expressed as

$$C_{tissue} = C_{t,ap}f_{t,ap} + C_{t,mp}f_{t,mp} + C_{t,ml}f_{t,ml} + C_{t,sl}f_{t,sl} + C_{t,w}f_{t,w} \quad (S-12)$$

where C_{tissue} is the PCBs concentration in tissue. $C_{t,ap}$, $C_{t,mp}$, $C_{t,ml}$, $C_{t,sl}$ and $C_{t,w}$ are the PCBs concentrations in tissue albumin proteins, muscle proteins, membrane lipids, storage lipids and water, respectively. $f_{t,ap}$, $f_{t,mp}$, $f_{t,ml}$, $f_{t,sl}$ and $f_{t,w}$ are the volume fractions of albumin proteins, muscle proteins, membrane lipids, storage lipids and water in tissue, respectively.

Assuming the partitioning equilibrium of PCBs in the steady-state tissue, the partitioning coefficients of the PCBs between biological components and water can be expressed as

$$K_{ap,w} = \frac{C_{t,ap}}{C_{t,w}}, K_{mp,w} = \frac{C_{t,mp}}{C_{t,w}}, K_{ml,w} = \frac{C_{t,ml}}{C_{t,w}}, \text{ and } K_{sl,w} = \frac{C_{t,sl}}{C_{t,w}} \quad (\text{S-13})$$

where $K_{mp,w}$ is the partitioning coefficient of PCBs between muscle protein and water.

Substituting Eqs. (S-13) into (S-12) gives the following

$$C_{tissue} = C_{t,w}(K_{ap,w}f_{t,ap} + K_{mp,w}f_{t,mp} + K_{ml,w}f_{t,ml} + K_{sl,w}f_{t,sl} + f_{t,w}) \quad (\text{S-14})$$

To have equal free concentration of PCBs *in vitro* and *in vivo*, $C_{free} = C_{c,w} = C_{t,w}$, the equivalent PCBs concentrations in tissues as wet weight, taking liver and plasma as examples, can be calculated as Eq. (5)

$$C_{liver} = C_{free}(K_{ap,w}f_{l,ap} + K_{mp,w}f_{l,mp} + K_{ml,w}f_{l,ml} + K_{sl,w}f_{l,sl} + f_{l,w}) \quad (\text{S-15})$$

and as Eq. (6)

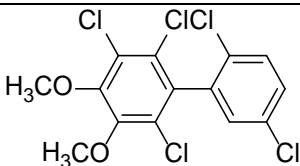
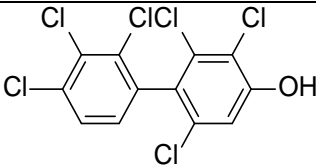
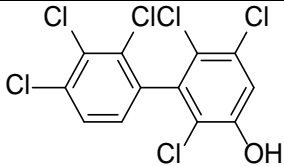
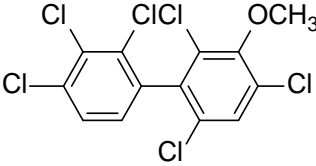
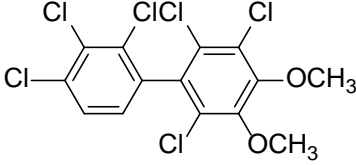
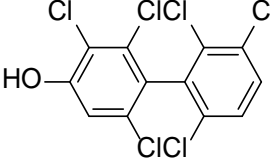
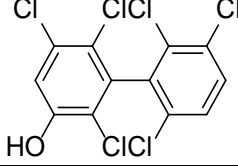
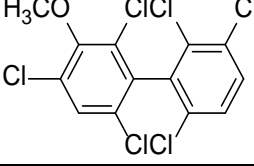
$$C_{plasma} = C_{free}(K_{ap,w}f_{p,ap} + K_{mp,w}f_{p,mp} + K_{ml,w}f_{p,ml} + K_{sl,w}f_{p,sl} + f_{p,w}) \quad (\text{S-16})$$

Table S1. Summary of the chemical structure, abbreviations, and the source of available hydroxylated or methoxylated standards used for the identification of potential OH-PCBs metabolites of PCB 91, PCB 95, PCB 132 and PCB 136.

Structures	Abbreviation	Source/Reference
	4-OH-PCB 91	4
	5-OH-PCB 91	4
	3-MeO-PCB 100	5
	4,5-di-MeO-PCB 91	4
	4-OH-PCB 95	4
	4'-OH-PCB 95	4
	5-OH-PCB 95	4
	3-MeO-PCB 103	5

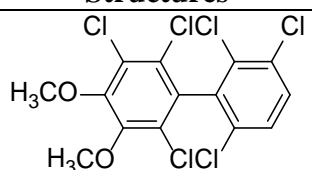
Note: The abbreviations for the PCB metabolite standards are based on the nomenclature proposed by Maervoet and co-workers.⁶

Table S1—continued. Summary of the chemical structure, abbreviations, and the source of available hydroxylated or methoxylated standards used for the identification of potential OH-PCBs metabolites of PCB 91, PCB 95, PCB 132 and PCB 136.

Structures	Abbreviation	Source/Reference
	4,5-di-MeO-PCB 95	4
	4'-OH-PCB 132	4
	5'-OH-PCB 132	4
	3'-MeO-PCB 140	5
	4',5'-di-MeO-PCB 132	4
	4-OH-PCB 136	7
	5-OH-PCB 136	7
	3'-MeO-PCB 150	7

Note: The abbreviations for the PCB metabolite standards are based on the nomenclature proposed by Maervoet and co-workers.⁶

Table S1—continued. Summary of the chemical structure, abbreviations, and the source of available hydroxylated or methoxylated standards used for the identification of potential OH-PCBs metabolites of PCB 91, PCB 95, PCB 132 and PCB 136.

Structures	Abbreviation	Source/Reference
	4,5-di-MeO-PCB 136	7

Note: The abbreviations for the PCB metabolite standards are based on the nomenclature proposed by Maervoet and co-workers.⁶

Table S2. Comparison of the enantiomeric fractions (EFs)^a of PCBs in the HepG2 cell culture system determined with different enantioselective columns shows a good concordance of the EF values.

Samples	Congeners	GC columns for chiral analysis ^b		
		CD ¹	CD ²	CB
Cells	PCB 91	0.77 (±0.03)		0.73 (±0.02)
	PCB 95	0.55 (±0.03)		0.50 (±0.01)
	PCB 132	0.69 (±0.01)	0.72 (±0.01)	
	PCB 136	0.55 (±0.01)	0.61 (±0.02)	0.61 (±0.02)
Dishes	PCB 91	0.68 (±0.01)		0.68 (±0.02)
	PCB 95	0.53 (±0.02)		0.51 (±0.02)
	PCB 132	0.63 (±0.01)	0.70 (±0.01)	
	PCB 136	0.68 (±0.08)	0.58 (±0.03)	0.68 (±0.04)
Media	PCB 91	0.41 (±0.02)		0.41 (±0.01)
	PCB 95	0.50 (±0.01)		0.51 (±0.01)
	PCB 132	0.44 (±0.01)	0.44 (±0.01)	
	PCB 136	0.47 (±0.01)	0.48 (±0.01)	0.48 (±0.01)
Dishes (cell-free)	PCB 91	0.54 (±0.01)	0.51 (±0.01)	0.51 (±0.01)
	PCB 95	0.50 (±0.01)	0.51 (±0.01)	0.48 (±0.02)
	PCB 132	0.47 (±0.01)	0.46 (±0.01)	
	PCB 136	0.45 (±0.01)	0.46 (±0.01)	0.45 (±0.03)
Media (cell-free)	PCB 91	0.49 (±0.01)		0.50 (±0.02)
	PCB 95	0.50 (±0.01)		0.50 (±0.02)
	PCB 132	0.50 (±0.01)		
	PCB 136	0.50 (±0.01)		
Standards	PCB 91	0.50 (±0.01)	0.50 (±0.01)	0.50 (±0.01)
	PCB 95	0.50 (±0.01)	0.50 (±0.01)	0.50 (±0.01)
	PCB 132	0.50 (±0.01)	0.50 (±0.01)	
	PCB 136	0.50 (±0.01)	0.50 (±0.01)	0.50 (±0.01)

^a Enantiomeric fractions (EFs) on the CD were calculated by the valley drop method⁸ as $EF = \text{Area } E_1 / (\text{Area } E_1 + \text{Area } E_2)$, where Area E_1 and Area E_2 are the peak areas of the first and second eluting atropisomers. The elution order of the two atropisomers of PCB 91 on the CB column is different from the elution order on the CD column.⁹ To account for the inversion in the elution order and to allow the direct comparison of the EF values, EF values determined on the CB column are expressed here as $EF = \text{Area } E_2 / (\text{Area } E_1 + \text{Area } E_2)$.

^b Enantioselective analyses of PCBs were performed on an Agilent 6890 gas chromatograph (GC) equipped with a ⁶³Ni-μECD detector and CP-Chirasil Dex CB (CD) (25 m length, 250 μm inner diameter, 0.25 μm film thickness; Agilent, Santa Clara, CA, USA) or Cyclosil-B (CB) (30 m length, 250 μm inner diameter, 0.25 μm film thickness; Agilent) capillary columns. Analyses were performed with two different CD columns, CD¹ and CD². Helium was used as carrier gas at a constant flow rate of 3 mL/min.¹⁰⁻¹³ The temperature program for the atropselective analysis of PCB 91, PCB 95 and PCB 136 was as follows: initial temperature 50 °C for 1 min, 10 °C/min to 140 °C, hold for 170 min, 15 °C/min to 200 °C, and hold for 20 min. The column temperature

program for the atropselective analysis of PCB 132 was as follows: initial temperature 50 °C for 1 min, 10 °C/min to 160 °C, hold for 140 min, 15 °C/min to 200 °C, and hold for 20 min.

Table S3. Quality assurance/quality control (QA/QC) data for the quantitative and chiral analysis of the PCBs.

QA/QC data	Sample type (number of samples)	PCB 91	PCB 95	PCB 132	PCB 136
Linear range ^a [ng/mL]	Standards (n=8)	1-1000	1-1000	1-1000	1-1000
LODs ^b [ng]	Media and cells (n=5)	0.5	0.3	0.1	0.8
	Dishes (n=2)	0.09	0.06	0.04	0.06
Background levels ^c [ng]	Media (n=9)	0.8 (±0.7)	1.2 (±1.7)	0.2 (±0.3)	0.5 (±0.3)
	Cells (n=9)	0.5 (±0.8)	2.8 (±3.2)	0.1 (±0.1)	0.8 (±1.4)
	Dishes (n=8)	0.4 (±0.4)	0.6 (±0.5)	0.4 (±0.4)	0.8 (±0.9)
Recoveries of PCB 117 ^d [%]	Media (n=45)	88 (±8)			
	Cells (n=21)	82 (±6)			
	Dishes (n=32)	62 (±9)			
Resolution ^e	Racemic standards (n=4)	0.90 (±0.06)	0.87 (±0.06)	0.98 (±0.06)	0.79 (±0.09)
EF value ^f	Racemic standards (n=3)	0.50 (±0.01)	0.50 (±0.01)	0.50 (±0.01)	0.50 (±0.01)

^a The linear coefficients (R^2) of the calibration curves in a concentration range from 1 to 1000 ng/mL ranged from 0.998 to 0.999 for all the PCBs, including the surrogate standard (PCB 117) and internal standard (PCB 204).

^b The limits of detection (LOD) of PCBs were calculated from method blanks as $\text{LOD} = \text{mean blanks} + 3 \times \text{standard deviation blanks}$.^{14, 15}

^c The background PCB levels in media, cells, and dishes were calculated from all control samples incubated in parallel with PCBs exposed samples.

^d Recoveries of the surrogate recovery standard (PCB 117) from the media, cells, or dish samples.

^e The resolution of the PCB atropisomers (R_s) on the CD column were calculated as: $R_s = (t_{R_1} - t_{R_2}) / 0.5(BW_1 - BW_2)$, where t_{R_1} and t_{R_2} are the retention times of the first and second eluting atropisomers, respectively, and BW1 and BW2 are the baseline width of the first and second eluting atropisomers.¹⁶

^f The enantiomeric fraction (EF) of the racemic PCB standards on CD column were calculated as $\text{EF} = \text{Area } E_1 / (\text{Area } E_1 + \text{Area } E_2)$.

Table S4. The permutations of the system descriptors in HepG2 cell culture system used for the model calculations.^a

Items	Albumin protein content ($V_{m,ap}$, $\mu\text{L/mL}$) or ($V_{c,ap}$, $\mu\text{L}/10^6\text{cells}$)	Storage lipid content ($V_{m,sl}$, $\mu\text{L/mL}$) or ($V_{c,sl}$, $\mu\text{L}/10^6\text{cells}$)	Membrane lipid content ($V_{m,ml}$, $\mu\text{L/mL}$) or ($V_{c,ml}$, $\mu\text{L}/10^6\text{cells}$)	Water content ($V_{m,w}$, $\mu\text{L/mL}$) or ($V_{c,w}$, $\mu\text{L}/10^6\text{cells}$)
MEM	1.59	0 ^b	0 ^b	998.4
FBS	27.1	0.719 ¹⁷	0.566 ¹⁸	971.6
			2.81	969.4
		1.162 ¹⁸	0.566 ¹⁸	971.1
			2.81	968.9
HepG2	0.287	0.0224 ¹⁹	0.0969	2.65
		0.0324 ²⁰		2.65

^a Values without citation were obtained from reference ²¹. The values for the densities of protein, storage lipid, membrane lipid, and water were 1.4, 0.93, 1 and 1 mg/ μL , respectively.³ Based on the data sources, there are four permutations of the biological components for medium (MEM plus FBS), and there are two permutations of the biological components for HepG2 cells. Therefore, eight permutations were used for the model calculations referring to the standard deviations in Fig. 2b and 3a and the averages in Fig. 3b.

^b A value of zero was assumed for the lipid contents in the medium because the minimum essential medium (MEM) contains only a negligible amount of lipid.

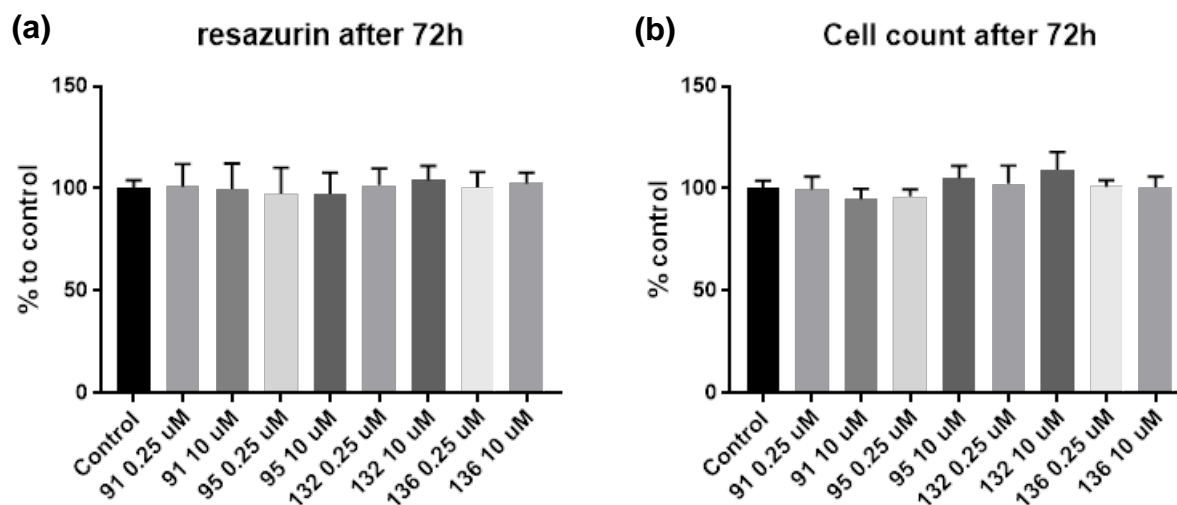


Fig. S1. The cytotoxicity of PCBs (PCB 91, PCB 95, PCB 132, and PCB 136) toward HepG2 cells by (a) resazurin method and (b) cell count method reveals no toxicity at the concentrations investigated (0.25 and 10 μ M). Briefly, HepG2 cells in 24-well plates with serum-free MEM were exposed to 0, 0.25 and 10 μ M PCB (0.1 % DMSO final concentration) for 72 h. Cells were either incubated with resazurin (50 μ M) in complete medium for 45 min after which fluorescence was measured with a microplate reader (resazurin assay) or detached and counted by Flow Cytometry (cell count). The assay was performed in duplicates at least 3-times, and the results are plotted as percent of control.

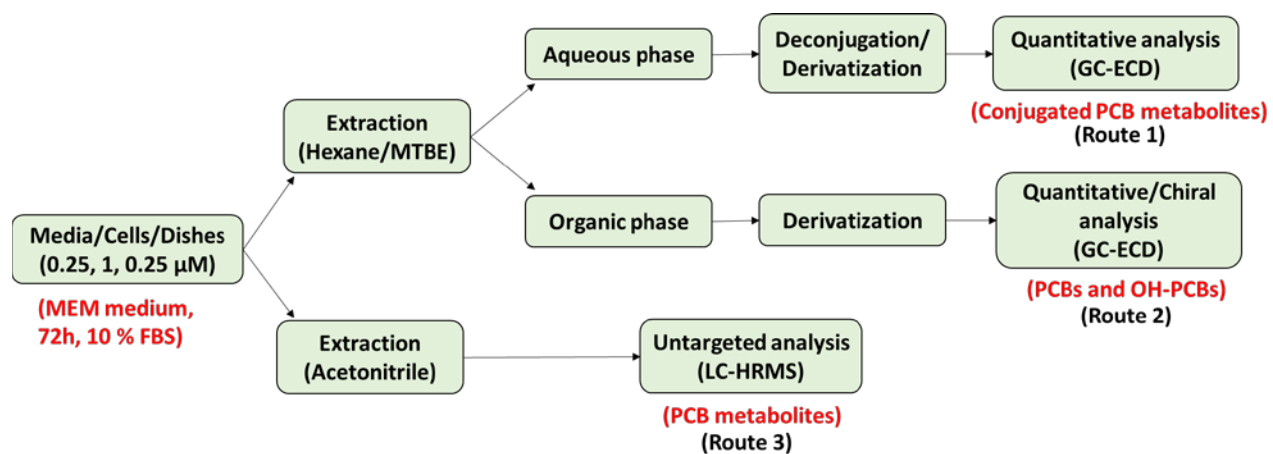


Fig. S2. Overall extraction workflow of PCBs and their metabolites from cell culture media, cell pellets, and dishes.

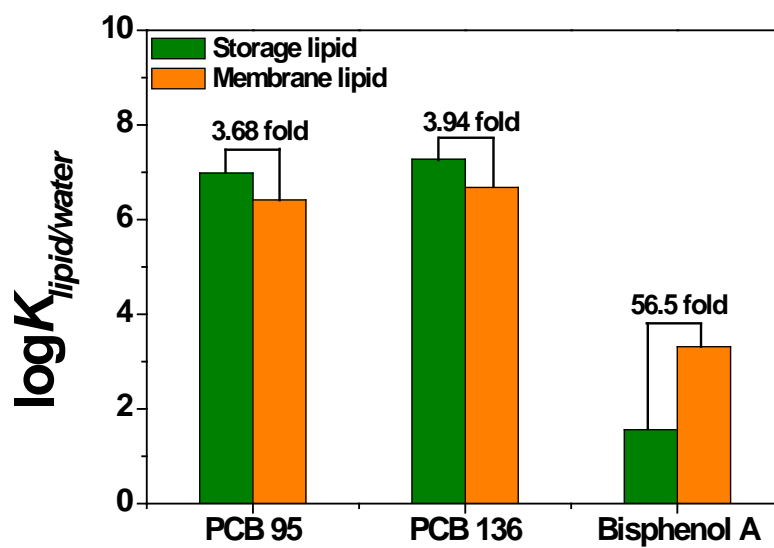


Fig. S3. The polyparameter linear free energy relationships (PP-LFER)³ predicted significant differences in the sorptive capacities (as partition coefficients) between storage lipids and membrane lipids for two PCBs, with the sorptive capacity being higher in storage than membrane lipids. In contrast, polar compounds, such as bisphenol A, have a higher sorptive capacity in the membrane than storage lipids.

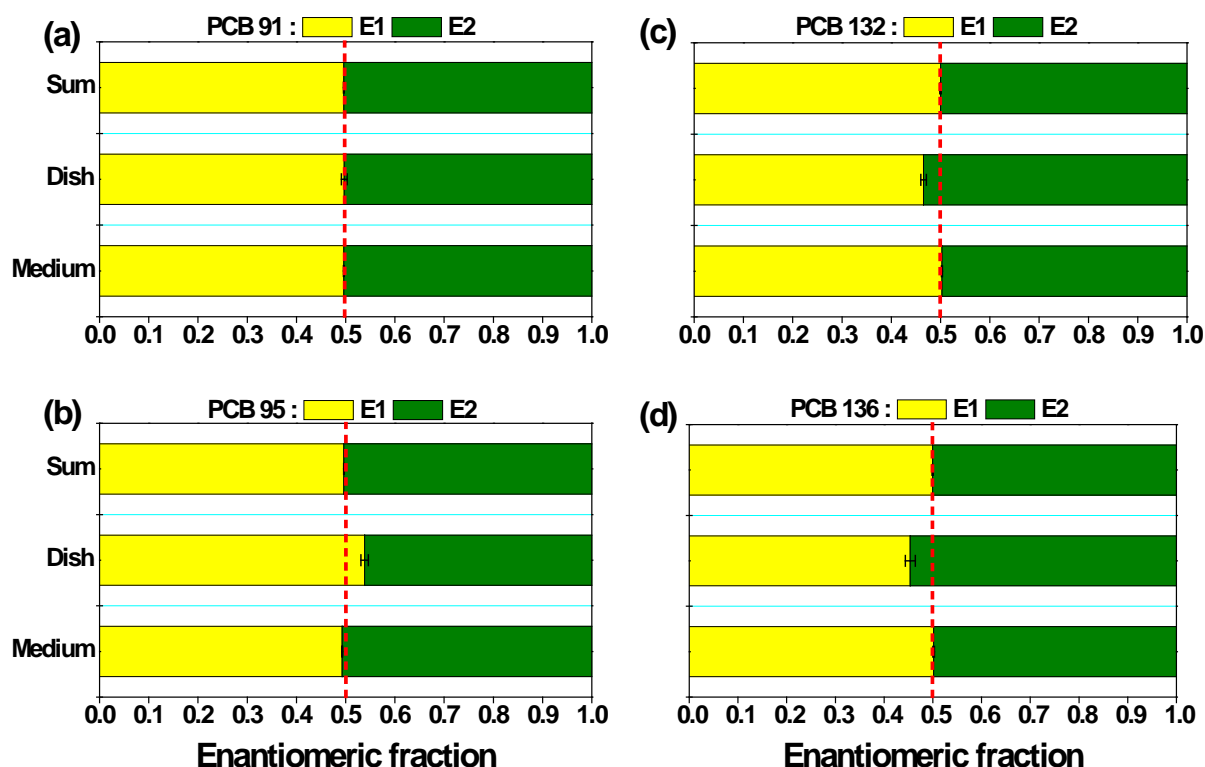


Fig. S4. The partitioning of (a) PCB 91, (b) PCB 95, (c) PCB 132 and (d) PCB 136 in a cell-free incubations is not enantioselective. The moderate atropisomeric enrichment observed in extracts from several cell culture dishes is likely due to the experimental error associated with the chiral analysis of samples with low PCB concentrations. Cell culture wells were incubated for 72 h with PCBs (0.25 μ M) in serum-free MEM, and the media and cell culture dish samples were extracted as described for incubations with HepG2 cells in the Experimental section.

Enantiomeric fractions (EFs) on the CD column were calculated by the valley drop method⁸ as $EF = \text{Area } E_1 / (\text{Area } E_1 + \text{Area } E_2)$, where Area E_1 and Area E_2 are the peak areas of the first and second eluting atropisomers. The elution order of the two atropisomers of PCB 91 on the CB column is different from the elution order on the CD column.⁹ To account for the inversion in the elution order and to allow the direct comparison of the EF values, EF values determined on the CB column are expressed here as $EF = \text{Area } E_2 / (\text{Area } E_1 + \text{Area } E_2)$. Enantioselective analyses of PCBs were performed on an Agilent 6890 gas chromatograph (GC) equipped with a ^{63}Ni - μ ECD detector and CP-Chirasil Dex CB (CD) (25 m length, 250 μ m inner diameter, 0.25 μ m film thickness; Agilent, Santa Clara, CA, USA). Helium was used as carrier gas at a constant flow rate of 3 mL/min.¹⁰⁻¹³ The temperature program for the atropselective analysis of PCB 91, PCB 95 and PCB 136 was as follows: initial temperature 50 $^{\circ}\text{C}$ for 1 min, 10 $^{\circ}\text{C}/\text{min}$ to 140 $^{\circ}\text{C}$, hold for 170 min, 15 $^{\circ}\text{C}/\text{min}$ to 200 $^{\circ}\text{C}$, and hold for 20 min. The column temperature program for the atropselective analysis of PCB 132 was as follows: initial temperature 50 $^{\circ}\text{C}$ for 1 min, 10 $^{\circ}\text{C}/\text{min}$ to 160 $^{\circ}\text{C}$, hold for 140 min, 15 $^{\circ}\text{C}/\text{min}$ to 200 $^{\circ}\text{C}$, and hold for 20 min.

References

1. McLean, M.R.; Robertson, L.W.; Gupta, R.C. Detection of PCB adducts by the P-32-Postlabeling technique. *Chem Res Toxicol* **1996**, *9*, 165-171.
2. Wu, X.; Zhai, G.; Schnoor, J.L.; Lehmler, H.J. Atropselective disposition of 2,2',3,4',6-pentachlorobiphenyl (PCB 91) and identification of its metabolites in mice with liver-specific deletion of cytochrome P450 reductase. *Chem Res Toxicol* **2019**.
3. Endo, S.; Brown, T.N.; Goss, K.U. General model for estimating partition coefficients to organisms and their tissues using the biological compositions and polyparameter linear free energy relationships. *Environ Sci Technol* **2013**, *47*, 6630-6639.
4. Joshi, S.N.; Vyas, S.M.; Duffel, M.W.; Parkin, S.; Lehmler, H.J. Synthesis of sterically hindered polychlorinated biphenyl derivatives. *Synthesis* **2011**, 1045-1054.
5. Kania-Korwel, I.; Vyas, S.M.; Song, Y.; Lehmler, H.J. Gas chromatographic separation of methoxylated polychlorinated biphenyl atropisomers. *J Chromatogr A* **2008**, *1207*, 146-154.
6. Maervoet, J.; Covaci, A.; Schepens, P.; Sandau, C.D.; Letcher, R.J. A reassessment of the nomenclature of polychlorinated biphenyl (PCB) metabolites. *Environ Health Persp* **2004**, *112*, 291-294.
7. Waller, S.C.; He, Y.A.; Harlow, G.R.; He, Y.Q.; Mash, E.A.; Halpert, J.R. 2,2',3,3',6,6'-hexachlorobiphenyl hydroxylation by active site mutants of cytochrome P4502B1 and 2B11. *Chem Res Toxicol* **1999**, *12*, 690-699.
8. Asher, B.J.; D'Agostino, L.A.; Way, J.D.; Wong, C.S.; Harynuk, J.J. Comparison of peak integration methods for the determination of enantiomeric fraction in environmental samples. *Chemosphere* **2009**, *75*, 1042-1048.
9. Kania-Korwel, I.; Lehmler, H.J. Assigning atropisomer elution orders using atropisomerically enriched polychlorinated biphenyl fractions generated by microsomal metabolism. *J Chromatogr A* **2013**, *1278*, 133-144.

10. Uwimana, E.; Li, X.S.; Lehmler, H.J. 2,2',3,5',6-Pentachlorobiphenyl (PCB 95) is atropselectively metabolized to para-hydroxylated metabolites by human liver microsomes. *Chem Res Toxicol* **2016**, *29*, 2108-2110.
11. Uwimana, E.; Maier, A.; Li, X.S.; Lehmler, H.J. Microsomal metabolism of prochiral polychlorinated biphenyls results in the enantioselective formation of chiral metabolites. *Environ Sci Technol* **2017**, *51*, 1820-1829.
12. Uwimana, E.; Li, X.S.; Lehmler, H.J. Human liver microsomes atropselectively metabolize 2,2',3,4',6-pentachlorobiphenyl (PCB 91) to a 1,2-shift product as the major metabolite. *Environ Sci Technol* **2018**, *52*, 6000-6008.
13. Uwimana, E.; Cagle, B.; Yeung, C.; Li, X.S.; Patterson, E.V.; Doorn, J.A.; Lehmler, H.J. Atropselective oxidation of 2,2',3,3',4,6'-hexachlorobiphenyl (PCB 132) to hydroxylated metabolites by human liver microsomes and its implications for PCB 132 neurotoxicity. *Toxicol Sci* **2019**, *171*, 406-420.
14. Marek, R.F.; Thome, P.S.; Herkert, N.J.; Awad, A.M.; Hornbuckle, K.C. Airborne PCBs and OH-PCBs Inside and Outside Urban and Rural US Schools. *Environ Sci Technol* **2017**, *51*, 7853-7860.
15. Persoon, C.; Peters, T.M.; Kumar, N.; Hornbuckle, K.C. Spatial distribution of airborne polychlorinated biphenyls in Cleveland, Ohio and Chicago, Illinois. *Environ Sci Technol* **2010**, *44*, 2797-2802.
16. Wu, X.A.; Pramanik, A.; Duffel, M.W.; Hryciak, E.G.; Bandiera, S.M.; Lehmler, H.J.; Kania-Korwel, I. 2,2',3,3',6,6'-Hexachlorobiphenyl (PCB 136) is enantioselectively oxidized to hydroxylated metabolites by rat Liver microsomes. *Chem Res Toxicol* **2011**, *24*, 2249-2257.
17. Cheever, M.; Master, A.; Versteegen, R.J. A method for differentiating fetal bovine serum from newborn calf serum. *BioProcessing Journal* **2017**, *16*.
18. Villard, P.H.; Barlesi, F.; Armand, M.; Dao, T.M.A.; Pascucci, J.M.; Fouchier, F.; Champion, S.; Dufour, C.; Ginies, C.; Khalil, A.; Amiot, M.J.; Barra, Y.; Seree, E. CYP1A1 induction in the

- colon by serum: involvement of the PPAR alpha pathway and evidence for a new specific human PPRE alpha site. *Plos One* **2011**, *6*.
19. Zhu, X.P.; Yan, H.M.; Xia, M.F.; Chang, X.X.; Xu, X.; Wang, L.; Sun, X.Y.; Lu, Y.; Bian, H.; Li, X.Y.; Gao, X. Metformin attenuates triglyceride accumulation in HepG2 cells through decreasing stearyl-coenzyme A desaturase 1 expression. *Lipids Health Dis* **2018**, *17*.
 20. Burdeos, G.C.; Nakagawa, K.; Kimura, F.; Miyazawa, T. Tocotrienol attenuates triglyceride accumulation in HepG2 cells and F344 rats. *Lipids* **2012**, *47*, 471-481.
 21. Fischer, F.C.; Henneberger, L.; Konig, M.; Bittermann, K.; Linden, L.; Goss, K.U.; Escher, B.I. Modeling exposure in the Tox21 in vitro bioassays. *Chem Res Toxicol* **2017**, *30*, 1197-1208.